Title: Enhanced metabolic detoxification is associated with fluroxypyr resistance in *Bassia scoparia*

Olivia E. Todd[1,2], Eric L. Patterson[3], Eric P. Westra[2,4], Scott J. Nissen[2], André Lucas Simões Araujo[2], William B. Kramer[2], Franck E. Dayan[2], Todd A. Gaines[2]*

[1]United States Department of Agriculture – Agriculture Research Service, Fort Collins, CO 80525, USA

[2]Department of Agricultural Biology, Colorado State University, Fort Collins, CO 80523, USA

[3]Department of Plant, Soil, and Microbial Sciences, Michigan State University, East Lansing, MI 48824, USA.

[4]Department of Plants, Soils & Climate, Utah State University, Logan, UT 84322, USA

*Author for correspondence: Todd Gaines, Department of Agricultural Biology, Colorado State University, Fort Collins, USA, 970-491-6824, Todd.Gaines@colostate.edu

ORCID IDs:

Olivia Todd: (ORCID 0000-0002-5727-1886)
Eric Patterson: (ORCID 0000-0001-7111-6287)
Eric Westra: (ORCID 0000-0003-3231-6985)
André Araujo: (ORCID 0000-0001-5331-0924)
William Kramer: (ORCID 0009-0009-0614-1457)
Franck Dayan: (ORCID 0000-0001-6964-2499)
Todd Gaines: (ORCID 0000-0003-1485-7665)

Abstract:

Auxin-mimic herbicides chemically mimic the phytohormone indole-3-acetic-acid (IAA). Within the auxin-mimic herbicide class, the herbicide fluroxypyr has been extensively used to control an agronomically problematic Great Plains tumbleweed, kochia (*Bassia scoparia*). A 2014 field survey for herbicide resistance in kochia populations across Colorado identified a putative fluroxypyr resistant population that was assessed for response to five different herbicides representing four different herbicide modes of action. These included fluroxypyr and dicamba (auxin-mimics), atrazine (photosystem II inhibitor), glyphosate (EPSPS inhibitor), and chlorsulfuron (acetolactate synthase inhibitor). The greenhouse screen identified that this kochia population was resistant to fluroxypyr and chlorsulfuron, but sensitive to glyphosate, atrazine, and dicamba. This population was designated Flur-R. Subsequent dose response studies determined that 75% of the Flur-R population survived 628 g ae ha^{-1} of fluroxypyr (4× the label application rate in wheat fallow, which is 157 g ae ha^{-1} at 1×). Flur-R was 40 times more resistant to fluroxypyr than a susceptible population (J01-S) collected from the same field survey (LD_{50} 720 and 20 g ae ha^{-1}, respectively). Auxin-responsive gene expression increased following fluroxypyr treatment in Flur-R, J01-S, and in a dicamba-resistant, fluroxypyr-susceptible line 9425 in an RNA-sequencing experiment. In Flur-R, several transcripts with molecular functions for conjugation and transport were constitutively higher expressed, such as glutathione S-transferases (GSTs), UDP-glucosyl transferase (GT), and ATP binding cassette transporters (ABC transporters). After analyzing metabolic profiles over time, both Flur-R and J01-S rapidly converted [^{14}C]-fluroxypyr ester, the herbicide formulation applied to plants, to [^{14}C]-fluroxypyr acid, the biologically active form of the herbicide, and three unknown metabolites. Formation and flux of these metabolites was faster in Flur-R than J01-S, reducing the concentration of phytotoxic fluroxypyr acid. One unique metabolite was present in Flur-R that was not present in the J01-S metabolic profile. Gene sequence variant analysis specifically for auxin receptor and signaling proteins revealed the absence of non-synonymous mutations affecting auxin signaling and binding in candidate auxin target site genes, further supporting our hypothesis that non-target site metabolic degradation is contributing to fluroxypyr resistance in Flur-R.

Key Words: Herbicide Resistance, NTSR, Synthetic Auxin

Significance Statement:

Herbicide resistance is an ever-present issue in weeds of cropping and rangeland systems. By understanding genetic mechanisms of resistance in individual cases of herbicide resistance, we can extrapolate important information such as how quickly resistance to a specific herbicide can spread. Every characterized herbicide resistance mechanism contributes to a working database used to address herbicide resistance in an agricultural or open-space setting. Knowing the exact mechanism of resistance helps researchers and industry members understand why herbicide applications are failing, and if resistant plants can still be controlled with other herbicide modes of action. In kochia line Flur-R, there is strong evidence to support a non-target site resistance mechanism, specifically herbicide degradation via increased enzymatic activity. Increased fluroxypyr degradation represents a novel resistance mechanism to fluroxypyr in the weed *Bassia scoparia*.

1. Introduction:

Kochia (*Bassia scoparia*) is an invasive, annual, broadleaf tumbleweed that is problematic in agronomic settings, open spaces, and rangeland in the U.S., specifically across the Great Plains. Herbicides, chemicals used to control unwanted plants, are the most prescribed method for kochia control in the U.S. Herbicide resistance in kochia is widespread, with resistance reported to multiple modes of action including ALS inhibitors (Group 2), glyphosate (Group 9), auxin-mimics (Group 4), and atrazine (Group 5), as well as cross-resistance to more than one Group 4 auxin-mimic herbicide (Geddes et al. 2021a; Kumar et al. 2019a; Kumar et al. 2019b). Furthermore, multiple resistance is increasingly common, where one population that is simultaneously resistant to more than one mode of action (Varanasi et al. 2015). The prevalence of glyphosate, atrazine, and ALS inhibitor resistant kochia has resulted in increased use of auxin-mimic herbicides for kochia management, mainly dicamba and fluroxypyr, in no-till fallow, wheat, and corn in the Great Plains region (Kumar et al. 2019b). While auxin-mimics have been used for more than 70 years, the evolution of resistance to this mode of action has lagged behind other herbicide modes of action (Busi et al. 2018). Despite this lag, recent evidence suggests that auxin-mimic resistance and multiple resistance in kochia is increasing (Geddes et al. 2022). Nine reports of auxin-mimic resistance across six U.S. states and two Canadian provinces have

described resistance in kochia populations as either resistant to dicamba alone, or resistant to both dicamba and fluroxypyr (Geddes et al. 2021b; Heap 2021; Jha et al. 2015; Kumar et al. 2019a). These herbicides mimic the phytohormone indole-3-acetic-acid (IAA) because they are chemically similar and induce auxin response gene transcription following application in weeds (Grossmann 2010; McCauley et al. 2020; Pettinga et al. 2018; Xu et al. 2022) (Figure 1).

IAA is an auxin plant growth hormone that is responsible for gravitropism and response to light stimuli; however, it impacts several other growth phenotypes as well (Zhao 2010). While auxins are involved in many cellular processes and signaling with other phytohormones, their function can be understood at the cellular level to primarily coordinate cell elongation (Perrot-Rechenmann 2010). In plants, auxin homeostasis is tightly regulated through a suite of biosynthesis pathways, cellular transport, feedback inhibition, oxidation and conjugation (Rosquete et al. 2012). When IAA reaches high levels in the plant, polar auxin carriers such as Pin-formed (PIN) efflux transporters, ATP binding cassettes (ABC class B) and Auxin resistant-1/like AUX1s influx carriers (AUX/LAX) help maintain IAA homeostasis and gradients (Cho and Cho 2013). Because the auxin-mimic herbicide fluroxypyr is chemically similar to and behaves like IAA, it is hypothesized that PIN, ABCs and AUX/LAX are able to direct the flow of fluroxypyr throughout the plant. In addition, fluroxypyr is a weak acid that can translocate in the plant based on its pKa and log Kow. Fluroxypyr also binds to Auxin signaling F-box 5, a member of the Transport inhibitor response1/Auxin signaling F-box (TIR1/AFB) receptor family (Lee et al. 2014). When applied, fluroxypyr and IAA act to stabilize the complex formed between AFB5 and the auxin dependent transcriptional regulator Indole-3-acetic acid inducible (Aux/IAA) proteins. Upon creation of this coreceptor-ligand complex, Aux/IAA proteins are ubiquitinated, degraded, and no longer negatively regulate Auxin Response Factors (ARF). These ARF proteins are seated on the Auxin Response Element (AuxRE) in auxin mediated gene promotors (Teale et al. 2006).

In Arabidopsis, plants treated with IAA or auxin-mimic herbicide (2,4-D) showed expression of early response genes such as Aux/IAAs and small auxin-up RNAs (SAURs). Other auxin induced genes included 1-aminocyclopropane-1 synthase (ACS), the first committed step in ethylene production and GH3, an auxin homeostasis gene. These genes were transcribed within minutes of high auxin perception (Guilfoyle 1999; Paponov et al. 2008; Raghavan et al. 2005). Many other phytohormone responses are also regulated by auxin perception, such as

Cytokinin oxidase (CXK6), brassinosteroid biosynthesis gene BAS1, and several gibberellin related genes. Regulation of multiple hormone related genes suggests that the relationship between phytohormones and auxin response is complex (Paponov et al. 2008). When the auxin-mimic herbicide fluroxypyr is applied to a plant, the resulting phenotypic response is stem-twisting, thickening, and lack of new growth at the meristem.

Herbicide resistance is categorized as either target site or non-target site (Gaines et al. 2020). Target site resistance is defined as a change (either in conformation or in expression) in a herbicide target protein. These changes often decrease herbicide binding affinity or in the case of overexpression, make it so the entire target protein pool is unable to be entirely inhibited (Murphy and Tranel 2019). LeClere et al. (2018) reported resistance to the auxin-mimic herbicide dicamba in kochia was due to the target-site mutation Gly127Asn in *IAA16*, which affects the formation of the coreceptor-ligand complex. More recently, Figueiredo et al. (2022b) characterized a 27-nucleotide deletion in the degron tail region of the gene encoding Aux/IAA2 that confers 2,4-D and dicamba resistance in Indian hedge mustard (*Sisymbrium orientale*). This deletion also affects formation and stability of the co-receptor-ligand complex. Non-target site resistance is broadly recognized as all other methods unrelated to target site resistance and is often exemplified by metabolic detoxification of an herbicide, herbicide sequestration, or a variant in a metabolism catalyzing enzyme which may have a downstream effect by reducing the efficacy of the herbicide (Delye 2013). Reduced translocation of 2,4-D via auxin transport proteins was reported by Goggin et al. (2019) in wild radish (*Raphanus raphanistrum*). A 2,4-D resistant population of waterhemp (*Amaranthus tuberculatus*) rapidly metabolized 2,4-D via CYP450 5-OH hydroxylation and subsequent amino acid and sugar conjugation reactions, which produced less phytotoxic metabolites that lost auxin signaling activity (Figueiredo et al. 2022a; Figueiredo et al. 2018). With both target site and non-target site resistance mechanisms described for auxin-mimic resistance (Todd et al. 2020), both possibilities are investigated in this study.

Our research objectives were to (1) **distinguish the application rate at which the fluroxypyr resistant kochia line (Flur-R) is resistant using a herbicide dose response,** (2) **determine whether fluroxypyr resistant kochia has any differences in absorption, translocation, or metabolism of fluroxypyr,** and (3) **identify potential candidate genes that may contribute to fluroxypyr resistance in Flur-R using RNA sequencing and alignment to the kochia genome assembly** (Hall et al. 2023).

In our work, a kochia population that was resistant to fluroxypyr converted fluroxypyr-ester into fluroxypyr-acid and subsequent metabolites at a faster rate than a susceptible line. Furthermore, the resistant line produced a metabolite that was not detected in the susceptible line. The results from an RNA-seq fluroxypyr-induced differential expression analysis show increased transcript expression of cellular transporters, cytochrome P450 monooxygenases (CYP450), glutathione s-transferases (GSTs) and UDP-glucosyl transferase (GTs) in the resistant plants. Taken together, these data suggest that metabolic detoxification of fluroxypyr may be the mechanism of fluroxypyr resistance in Flur-R.

2. Materials and Methods

2.1 Plant Materials

In 2014, 171 kochia (*Bassia scoparia)* populations were collected from a field survey conducted in eastern Colorado (Westra et al. 2019). These populations were screened at a single doses of dicamba, fluroxypyr, and glyphosate to test for resistance. One population, Flur-R, was found to have a few individuals (<2%) surviving a single fluroxypyr dose of 157 g ae ha^{-1} (label rate for use in wheat) (Starane Ultra, Dow Agrosciences, Indianapolis, IN). Survivors at 157g ae ha^{-1} were selected and allowed to bulk pollinate. After two more generations of selection at both 157g ae ha^{-1} and 314 g ae ha^{-1}, the surviving individuals were cross-pollinated. The progeny of these plants were found to be uniformly resistant to 314g ae ha^{-1} fluroxypyr. During the bulking stages, groups of three to four plants were planted in one gallon pots and covered with a pollination bags to allow for cross-pollination. Seed was harvested per pot, hand threshed and cleaned using an air-column blower. Seeds were stored at 4 C and planted in the spring in a greenhouse maintained at 25 C with a 16 h photoperiod. An inbred dicamba resistant/fluroxypyr susceptible population (9425) homozygous for a G127N mutation in the *IAA16* gene (LeClere et al. 2018; Preston et al. 2009) and a fluroxypyr susceptible field population from the 2014 eastern Colorado field study (J01-S) (Westra et al. 2019) were included in the dose response and single dose screening as susceptible controls.

2.2 Fluroxypyr and Dicamba Dose Response

Seeds of Flur-R, J01-S, and 9425 were planted in 1.5 cm^2 280-count plug flats. Plants were sub-irrigated and thinned down to one plant per cell. When plants were approximately 4-5

cm tall, uniform seedlings were transplanted to 4 cm^2 plastic pots containing SunGro potting mix (American Clay Works Supply, Denver, CO). Plants kept in the greenhouse under conditions previously described. They were sub-irrigated once a week for three weeks until the plants reached 10 cm height. A randomized complete block design was used for each dose, with one plant per pot, four plants per dose and three replications for a total of 12 treated plants. The dose response for fluroxypyr included the following eight rates: 0, 20, 40, 80, 157, 314, 628, and 1,256 g ae ha^{-1} fluroxypyr (Starane Ultra, Corteva Agrisciences, Indianapolis, IN). The dicamba doses included 0, 35, 70, 140, 280 (1x), 560, 1120, and 2240 g ae ha^{-1} (Engenia, BASF, Research Triangle Park, NC) mixed with Induce (NIS, 0.25% v/v, Helena Agri-Enterprises, LLC, 24330 US-34 Greely, CO 80631). Applications were made with a DeVries Generation 4 Research Track Sprayer (DeVries Manufacturing, Hollandale, MN, 86956) equipped with a TeeJet (TeeJet Technologies, 1801 Business Park drive, Springfield, IL) 8002EVS nozzle calibrated to deliver 187 L ha^{-1}. Plant height was measured by recording the distance in centimeters from the soil surface to the newest leaf in the apical meristem before treating and was measured again 30 days after treatment. Survival (dead or alive) was also recorded 30 days after treatment. An individual was considered "dead" if it displayed severe epinasty, stem thickening, yellowing, and had no new growth at the axillary or primary meristems after 30 days. An individual was considered "alive" if it displayed minimal to no epinasty or stem thickening, had no yellowing, and had new growth at the axillary or primary meristems after 30 days. Percent survival was chosen for fluroxypyr resistance assessment because while percent change in height can accurately differentiate between resistant and susceptible plants, for this population it did not accurately represent an actively growing plant in the individuals where axillary meristem growth was the primary source of regrowth.

For data analysis, the response variable "Percent Survival" was created by transforming binary data according to the equation:

$$Y = \left(\frac{N_1}{N_{total}}\right) * 100 \text{ [1]}$$

Where Y is the percent survival at each calculated dose, N_1 is the number of individuals marked as "alive" according to the parameters above. N_{total} is the number of individuals per rate.

The response variable "Percent Change in Height" over 30 days was normalized using the following equation:

$$Y = (X_{\Delta Height}/A_{Avg}) * 100 \text{ [2]}$$

Where *Y* is the change in height as a percent of the 0 g ae ha^{-1} rate for each population. $X_{\Delta Height}$ is the change in height in centimeters for an individual from day 0 to 30 days, and A_{Avg} is the average change in height for individuals at the 0 g ae ha^{-1} rate for the population being measured. The model used by the drm package in R did not converge for the J01-S or 9425 lines using "Percent Change in Height (% control)" as a response variable due to the non-sigmoidal behavior of the curve, so "Percent Survival" data were analyzed using a three-parameter log-logistic model (Knezevic et al. 2007), which was the best model by a lack-of-fit test from the drc package in R (R Core Team 2020) with the equation:

$$Y = \frac{d}{1+exp\,[b\,(log\,[(x-\,log)\,(e)])]} \quad [3]$$

where *Y* is the percent survival 30 days after treatment, *d* is the upper limit parameter, *b* is the regression slope, *x* is the dose of either fluroxypyr or dicamba in g ae ha^{-1} and *e* is the dose at which 50% mortality is achieved (Table 1). The data were averaged per treatment and the standard error of the mean is presented per dose. "Rate" and "Population" were used as predictor variables and the experiment was repeated.

2.3 Glyphosate, Atrazine, and Chlorsulfuron Single Rate Screening

Flur-R and J01-S seeds were planted in 4 cm^2 plastic pots containing SunGro potting mix. Plants were sub-irrigated and thinned down to one plant per cell and kept at greenhouse conditions previously described. When plants were approximately 7 cm in height, plants were treated with one of the following herbicides (n=72 plants per herbicide): atrazine (Aatrex 4L, Syngenta, Greensboro, NC, 2240 g ai ha^{-1}, 1% crop oil concentrate), chlorsulfuron (Telar XP, Bayer CropScience, St. Louis, MO, 137 g ai ha^{-1}), or glyphosate (RoundUp Powermax, Monsanto Company, St. Louis, MO, 870 g ae ha^{-1}, 2% w/v ammonium sulfate). All treatments were applied with the same equipment and nozzle type described above. Survival (dead or alive) was assessed 30 days after treatment. In a *post hoc* analysis, a random number generator was used to assign each of the 72 individuals to one of three blocks with n=24 to serve as replicates. Standard error of the mean was calculated using the standard deviation from this analysis.

2.4 Kompetitive allele specific PCR (KASP)

Approximately 200 mg of meristem tissue was harvested from 20 individuals each of Flur-R and 5 individuals for the mutant and wild type checks. Flur-R individuals were verified as

resistant by spraying with 157 g ae ha^{-1} fluroxypyr. Tissue was put into a 1.5 mL Eppendorf tube and flash frozen in liquid nitrogen. DNA extraction protocol was adapted from Aboul-Maaty and Oraby (2019) using the established CTAB method. DNA purification was checked using a NanoDrop2000 and diluted to 5 ng uL^{-1}. The FAM fluorophore (in bold) was added to the forward primer specific to the G127N *IAA16* double mutation (allele specific sequence in italics) endowing a protein change from wildtype GWPPV to NWPPV in kochia described by LeClere et al. (2018) (5'**GAAGGTGACCAAGTTCATGCT**TGTTCTTCAGGACACAAGTTGTA*AA*) and the HEX fluorophore (in bold) was added to the forward primer specific to the wild type sequence (in italics) (5'**GAAGGTCGGAGTCAACGGATT**TGTTCTTCAGGACACAAGTTGTA*GG*). One universal reverse primer (5'AGTTTGATCATCGGACGTCTTCTT) and the forward primers were designed with IDT PrimerQuest. The KASP protocol and specific mix ratios are published on protocols.io at dx.doi.org/10.17504/protocols.io.dm6gpj9njgzp/v1. Fluorescence was recorded at the end of every cycle. Fluorescence at the 35^{th} cycle was used for the allelic discrimination data. Data were plotted using GraphPad Prism version 8.4.2. Genotypes were assigned manually as homozygous wildtype, homozygous mutant, or heterozygous.

2.5 Plant Material for Fluroxypyr Absorption, Translocation, and Metabolism

Seeds from Flur-R and J01-S were sown into plug flats filled with SunGro potting mix and grown on a light shelf under 700 µmol m^{-2} s^{-1} of light at 25 C. When the plants reached 3-4 cm tall, 50 seedlings from each line were washed of soil in the roots and transplanted into a 25 mL Eppendorf tube filled with silica sand and fertilized with three granules of Osmocote. Uniform plants that were 4-5 cm tall and had recovered from transplanting were used in all subsequent absorption, translocation and metabolism experiments.

2.6 Fluroxypyr Absorption and Translocation

Flur-R (n=24) and J01-S (n=24) plants were sprayed with 157 g ae ha^{-1} fluroxypyr using a track sprayer as described in section 2.2. The third and fourth youngest leaves were protected from the broadcast application using aluminum foil. Immediately after applying fluroxypyr, the covered leaves of were treated with five 1 µL drops of the spray solution spiked with 3.1 kBq [^{14}C]-fluroxypyr. Absorption and translocation were monitored over a 196 h time course, with

time points at 6, 12, 24, 48, 96 and 192 hours after treatment (HAT). Four Flur-R and four J01-S were harvested at each timepoint. Treated leaves were removed and washed in 5 mL 90% water, 10% methanol, and 0.5% non-ionic surfactant. The leaf wash was mixed with 10 mL scintillation cocktail (Ecoscint XR) and radioactivity was measured using a liquid scintillation counter (LSC) (TRI-CARB 2300TR, Packard Instruments Co., USA). Roots were washed with 5 mL water. Root wash and the silica sand rinse solution were vortexed for 3 seconds, and 1 mL of the root wash and sand rinse mixture was added to 10 mL scintillation cocktail to measure root exudation. Plants were sectioned and separated as follows: above treated leaves, treated leaves, below treated leaves, and root biomass. Each separate plant part was dried and oxidized using a biological oxidizer (Model OX500, R. J. Harvey Instrument Co., USA). The released ^{14}C-CO_2 was collected by a ^{14}C trapping cocktail (OX161, R.J. Harvey Instrument Co., USA). Radioactivity was quantified by LSC. One individual per timepoint was left intact, dried, and used for phosphor imaging (Typhoon Trio, GE Healthcare). Dried plants were separated and oxidized in the same manner as described above after imaging.

The experiment was repeated. Percent absorption and translocation was calculated as follows from Figueiredo et al. (2018) and maximum percent absorption was determined using a method described by Kniss et al. (2011) in R.

$$\%H_{\text{abs}} = [(^{14}\text{C ot}) / (^{14}\text{C ot} + {}^{14}\text{C wl})] \times 100$$

$$\%H_{\text{tr}} = 100 - [(^{14}\text{C al}) / (^{14}\text{C al} + {}^{14}\text{C ot}) \times 100]$$

Where "$\%H_{\text{abs}}$" is percent absorption of [^{14}C]-fluroxypyr ester, "^{14}C ot" is the sum DPM from the oxidation of all plant parts and "^{14}C ot + ^{14}C wl" is the sum DPM from the oxidation of all plant parts and counts washed from the treated leaf. For herbicide translocation studies, "$\%H_{\text{tr}}$" is percent translocation of [^{14}C]-fluroxypyr ester out of the treated leaf through the rest of the plant, "^{14}C al" is the DPM [^{14}C]-fluroxypyr ester counted in the treated leaf.

2.7 Fluroxypyr Metabolism

Fluroxypyr metabolism was evaluated by treating Flur-R and J01-S plants as pervioulsy described. Plants were sprayed with fluroxypyr while two leaves were protected from the spray solution. Those protected leaves were then treated with five 1 µL drops of the spray solution spiked with 25 kBq [^{14}C]-fluroxypyr. The time course was the same as previously described with four repetitions per timepoint. Treated leaves were removed and washed as previously described.

The washed treated leaves were placed back with the remaining whole-plant tissue and flash frozen in liquid nitrogen. Whole plants were then finely ground in a glass test tube with liquid nitrogen and a glass rod. Five mL extraction solution (90% water, 9% acetonitrile, 1% acetic acid) was added to each tube and samples were shaken for 30 min. The extraction solution was tranferred to a 0.45 µm filter tube which was rinsed with an additional 5 mL extraction buffer and centrifuged at ~2600×g for 10 min to separate liquid from ground plant material. The extraction buffer that passed through the 0.45 µm filter was transferred to a C-18 cartridges preconditioned with 1 mL 100% acetonitrile (Waters Co., Sep-Pak Plus). Using a vacuum manifold, the extraction buffer was pulled throught the solid phase extraction cartridge. Bond solutes were eluted from the C18 cartridge with 5 mL 100% acetonitrile and samples were then evaporated to dryness in a fume hood. Solvent A (500 µL) consisting of 10% acetonitrile and 1% formic acid was added to each tube. Each sample was filtered through 25 µm nylon filters (Nalgene) into an injection vial with a 500 µL insert. High Pressure Liquid Chromatography (HPLC) (Hitachi Instruments, Inc.,) was used to separate radiolabelled fluroxypyr-ester, fluroxypyr acid and metabolites.. The HPLC was equipped with a C-18 column (4.6 mm by 150 mm column, Zorbax Eclipse XDB-C18, Agilent Technologies) and inline radio-detector (FlowStar LB 513, Berthold Technologies GmbH & Co.) with a YG-150-U5D solid scintillation flow cell (150 µL). The injection volume was 200 µL. Radiolabelled fluroxypyr-ester had a retention time of 9.8 min, while fluroxypyr acid had a retention time of 2.8 minutes (protocol published on protocols.io at dx.doi.org/10.17504/protocols.io.kqdg39yopg25/v1).

2.8 Plant Material and Treatment for RNA Sequencing

Seeds from lines Flur-R, 9425, and J01-S were treated as described above, in similar growing conditions. When the plants reached 7-10 cm tall, 20 of the most uniform seedlings from each line were treated as follows: All plants were sprayed with water and 0.01 g meristem tissue was harvested for the untreated RNA-sequencing timepoint. Tissue was flash frozen in liquid nitrogen. The same twenty plants per line were treated 24 h later with 157 g ae ha^{-1} fluroxypyr, the labeled rate to control kochia. Approximately 0.01 g of meristem tissue was harvested at 3 and 10 h after fluroxypyr treatment for the remaining two RNA-sequencing timepoints. Herbicide and water applications were made with a track sprayer as described in section 2.2. All plants were in the vegetative stage, except for one Flur-R individual and three

J01-S individuals, which were in the early flowering stage at the time of tissue harvest. After 30 days, resistance response was measured and four individuals per timepoint per line were selected for RNA-sequencing.

2.9 RNA Extraction, Sequencing and Quantification

The RNA-sequencing experiment was conducted first by extracting total RNA following the protocols in the QIAGEN RNeasy plant mini kit in six batches containing two individuals of each line to minimize batch effects. The kit was used to extract RNA from the top three fully expanded apical meristem leaves of Flur-R, 9425, and J01-S of 5-7 cm tall kochia at 0, 3, and 10 h after 157 g ai ha^{-1} fluroxypyr treatment. Final elution volume was 30 µL. Total RNA samples were diluted to a range of 500-10,000 pg μL^{-1} for quality check using an Agilent ScreenTape. Samples that had a RIN score above 6 were submitted to BGI Technologies for quality check following their sample submission guidelines. Following quality check by BGI, 30 samples were used for sequencing. From the total RNA, mRNA enrichment was performed by rRNA depletion. Reverse transcription of the mRNA was performed with random N6 primers followed by end repair and A-tail and adapter ligation to the fragments. After PCR amplification, single strand separation and single-strand circularization were conducted to sequence paired end 100 base pair fragments with the BGISEQ sequencing platform. In total, 2.8 billion reads were produced, resulting in 92-97 million 100 bp reads per sample.

2.10 Differential Expression and Variant Analysis

Individual fasta files were uploaded to the remote research computing resource SUMMIT (Jonathon Anderson 2017) and files were quality checked with FastQC (version 0.11.9). Adapters were trimmed by BGI Bioinformatics company after sequencing and quality check. Reads were aligned to the *Bassia scoparia* coding sequence version 2 (Hall et al. 2023) using HISAT2 (version 2.2.0 (Kim et al. 2019)). Reads were assigned to features using featureCounts in the Subread package (version 2.0.1, Liao et al. 2014). Differential expression was conducted with resultant reads for each gene feature using the DESeq2 package (version 1.28.1) in the statistical software R (version 4.0.2 (R Core Team 2020)). Reads were transformed to logarithmic fold change log2 and compared across biological replicates for each population. For each population, the untreated condition was compared to either the 3 or 10 h timepoint to

363 determine expression. Mean normalized counts per gene, an adjusted pvalue of < 0.05, and log2
364 fold change > 0.5 were the pre-filtering parameters used by DESeq2 for optimal significant
365 genes below the false discovery rate (FDR) of <0.05.
366 Sorted and indexed bam files were run through the variant calling software Platypus
367 (version 0.8.1 (Rimmer et al. 2014)) to detect single and mono-nucleotide polymorphisms, short
368 and long indels, as well as chromosome rearrangement. The output file was used with the
369 software SnpEff (version 4.3 (Cingolani et al. 2012)) to annotate the variants called from
370 Platypus and to provide effect predictions. Specific genes annotated with involvement in the
371 auxin signaling pathway or metabolic herbicide resistance were targeted for variant analysis by
372 checking chosen genes against a merged variant file for all individuals of each population.
373 Presence or absence of variants were validated with Integrative Genomics Viewer (IGV)
374 (Robinson et al. 2017).
375
376 **3. Results**
377 *3.1 Fluroxypyr and Dicamba Dose Response*
378 Flur-R was confirmed to be fluroxypyr resistant based on change in height (Figure 2A)
379 and percent survival (Figure 2B) at 30 days after treatment (DAT), with 75% survival up to 628
380 g ae ha^{-1} of fluroxypyr (Figure 2B). Flur-R was approximately 40 times more resistant than the
381 susceptible population J01-S and 36 times more resistant than 9425 (Table 1). The population
382 9425, which was previously reported to be fluroxypyr resistant (LeClere et al. 2018) was
383 subsequently shown to have weak fluroxypyr resistance (Wu et al. 2020). Our results show 9425
384 had less than 25% survival at 157 g ae ha^{-1} fluroxypyr (Figure 2B) and had similar reduction in
385 height as the known susceptible population J01-S (Figure 2A). The LD_{50} ratios for J01-S and
386 9425 were not statistically different from 1, indicating that 9425 is not resistant to fluroxypyr at
387 field rates. Furthermore, Flur-R was susceptible to dicamba (Figure 2C), with 8% survival at 70
388 g ae ha^{-1} and an LD_{50} of 56 g ae ha^{-1}. Flur-R is approximately seven times more susceptible than
389 9425 to dicamba (Table 1).
390
391 *3.2 Glyphosate, Atrazine, and Chlorsulfuron Single Rate Screening*
392 No Flur-R or J01-S individuals survived glyphosate (870 g ae ha^{-1}) or atrazine (2240 g ai
393 ha^{-1}) treatments; however, 94% (± 0.5%) of the Flur-R population and 7% (± 0.5%) of J01-S

individuals survived chlorsulfuron (137 g ai ha^{-1}). This indicates that there is multiple resistance in this fluroxypyr resistant population. Two target site mutations were identified in a SNP analysis of RNA-sequencing data that confer ALS resistance, including a proline 197 to threonine mutation and a tryptophan 574 to leucine mutation in the *ALS* gene (Tranel and Wright 2002) (SI Figure 1).

3.3 KASP

Kompetitive allele specific PCR (KASP) was used to genotype individuals using allelic discrimination to determine whether or not Flur-R individuals contained the G127N *IAA16* mutation reported by LeClere et al. (2018). Specific fluorophore sequences were assigned to each forward primer, which generated a fluorescent signal to determine which allele was present in the kochia DNA sample. Relative Fluorescence Units (RFU) were measured to determine which of the fluorophore sequences amplified for each sample (Figure 3A). Of the twenty verified fluroxypyr-resistant individuals tested from the Flur-R population, 10 individuals displayed high RFU for the HEX labeled primer, indicating they had a homozygous wildtype genotype. There were six individuals that displayed approximately equal RFU for both alleles, indicating heterozygous individuals for G127N *IAA16*. Two known susceptible wild type controls were included (kochia lines J01-S, 7710), as well as one homozygous mutant resistant control (9425). These results indicate that the asparagine-127 *IAA16* mutant allele is not essential for fluroxypyr resistance, as most individuals were homozygous for the wildtype glycine-127 *IAA16* allele and were resistant to fluroxypyr. The dicamba resistance asparagine-127 *IAA16* allele is present and segregating in the Flur-R population.

3.4 Fluroxypyr Absorption, Translocation, and Metabolism

We investigated differences in [^{14}C]-fluroxypyr ester absorption and translocation between fluroxypyr-resistant line Flur-R and fluroxypyr-susceptible J01-S. For each of the two lines, two meristem leaves per individual were treated with [^{14}C]-fluroxypyr ester. Differential absorption and translocation were investigated by partitioning all individuals into four plant sections. Radioactivity was quantified in each section using biological oxidation and liquid scintillation counting. Maximum percent absorption of ~3.33 kBq [^{14}C]-fluroxypyr ester for Flur-R was 91.99% ($\pm$3.14), and for J01-S was 85% ($\pm$3.13). Percent recovery of radioactivity

was >75% for all samples, except two samples per line at 192h which were ≥50%. No significant differences in maximum absorption between Flur-R and J01-S were found (pvalue = 0.155) (Figure 4A). The time (h) after treatment in which 90% of the herbicide is absorbed based on the model in R was not statistically different between 12 h (± 2.15) for Flur-R, and 9.7 h (± 2.34) for J01-S (pvalue = 0.47). There were no differences in translocation of [^{14}C]-fluroxypyr ester from the treated leaf to the rest of the plant between Flur-R and J01-S (Figure 4B and C).

Whole plant metabolites were extracted for [^{14}C]-fluroxypyr ester metabolism studies. Analysis of metabolites was conducted using an HPLC equipped with a C18 column. [^{14}C]-fluroxypyr ester and acid standards were analyzed using an HPLC to determine retention time. Analysis of the proportion of [^{14}C]-fluroxypyr ester in each population showed a significant difference at 12 h. The overall proportion of [^{14}C]-fluroxypyr ester was lower in Flur-R than J01-S, supporting rapid conversion from the [^{14}C]-fluroxypyr ester to biologically active [^{14}C]-fluroxypyr acid or other [^{14}C]-fluroxypyr metabolites (Figure 5). In Flur-R, the high amount of [^{14}C]-fluroxypyr acid at 12 h was significantly reduced by 48 h, showing rapid conversion from to other fluroxypyr metabolites (Figure 5B). At 96 h and 192 h, the proportion of unknown metabolites numbered 4 and 2 were higher or uniquely present in Flur-R compared to J01-S (Figure 5D and F). This suggests that formation and flux of these metabolites is catalyzed by a process that is more active in Flur-R than J01-S and may play a role in reducing concentrations of phytotoxic [^{14}C]-fluroxypyr acid.

3.5 Differential Expression Analysis

To analyze the transcriptome of Flur-R, we sequenced RNA from 4 plants each of fluroxypyr resistant Flur-R, and two fluroxypyr susceptible lines J01-S and 9425. BGI Seq was used to obtain between 91 and 95 million clean reads per sample (BGI Bioinformatics, San Jose, CA). Q20 scores were between 96–98%. Alignment was made to the coding sequence of the *Bassia scoparia* genome assembly version 2 (Hall et al. 2023) using HISAT2 (version 2.1.0), and alignment ranged between 59 - 63% for all individuals. Percent unmapped reads ranged between 46 – 51%, and percent uniquely mapped genes ranged from 43 – 48%. Approximately 4% of reads were multi-mapped (SI Table 1). Following alignment and differential expression with DESeq2, a Wald test was used to obtain p-values, which were adjusted using the Benjamini-Hochberg method. Filtering parameters included samples with an adjusted p-value < 0.05 and

log2 fold change > 0.5. The false discovery rate (FDR) was < 0.05. We identified 231 unique genes that had higher expression in Flur-R compared to both 9425 and J01-S at the untreated timepoint (Figure 6). Because we identified differential metabolism in Flur-R, we explored the hypothesis that genes related to herbicide metabolism may have differential regulation or be highly expressed at the untreated timepoint in Flur-R. Of these 231 highly expressed genes in Flur-R at the untreated timepoint, there were six ABC transporters of both class B and G, including genes homologous to *ABCG31-like* (*Bs.00g217020.m01*), two similar ABCB28 annotated genes (*Bs.00g454440.m01, Bs.00g282300.m01*), two isoforms of *ABCG34* (*Bs.00g184080.m01, Bs.00g184080.m02*), and *ABCG29* (*Bs.00g251290.m01*). There were five CYP450 annotated genes between two families, the CYP71 family (*CYP82D47* [*Bs.00g486870.m01*], *CYP96A15* [*Bs.00g541440.m01*], *CYP71D10/11* [*Bs.00g051830.m01*], Ent-kaurene oxidase [*Bs.00g184110.m01*],) and the CYP85 family (*CYP90C1/D1* [*Bs.00g245700.m01*]). Several types of glucosyltransferases were expressed, such as UDP-glucosyltransferase 73B2 (*Bs.00g142060.m01*), two isoforms of UDP-glucuronosyl/UDP-glucosyltransferase 89A2-like (*Bs.00g480980.m01, Bs.00g480980.m02*), and UDP-glycosyltransferase 87A1 (*Bs.00g061050.m01*) (Table 2).

When analyzing the treated timepoints within Flur-R, J01-S, and 9425, 188 (3 h after treatment [HAT] vs untreated) and 300 genes (10 HAT vs untreated) were upregulated in response to fluroxypyr treatment in all three lines (Figure 7A and B). Of those shared upregulated genes, auxin responsive genes encoding proteins such as GH3.2 (*Bs.00g477580.m01*), Ethylene responsive transcription factors, Small auxin-up RNAs (SAURs), Aux/IAAs, and ACS (*Bs.00g478760.m01*) were among them, indicating that all three kochia lines perceived fluroxypyr and had transcriptional activation of these auxin responsive genes following fluroxypyr treatment (SI Figure 2). The Ethylene responsive transcription factors, *GH3*, and *ACS* were in the top 20 genes with the highest fold change through the 3 HAT vs untreated and 10 HAT vs untreated timepoints in Flur-R, J01-S, and 9425 (Tables 3, 4, 5). Two isoforms of the IAA cellular transporter PIN were upregulated in 9425 at 10 HAT (*Bs.00g190770.m01* and *Bs.00g190770.m02*), but the response in Flur-R and J01-S did not meet the differential expression filtering criteria and therefore the response was not statistically different following fluroxypyr treatment (Figure 8). Within the Flur-R line at 3 HAT vs untreated, there were 278 uniquely upregulated genes and 303 at 10 HAT vs untreated (Figure

7A and B). Some unique auxin-induced genes such as *SAURs* and *ARF11* were upregulated in Flur-R, but six additional ABC transporters of class G, two ABC transporters of class C, one ABC transporter of class A, six additional UDP-glucosyltransferases (GTs), and three sugar transporters were upregulated following fluroxypyr treatment (expression data not shown). CYP450s *CYP81B2* (*Bs.00g431990.m01*), *CYP82D47*, and *CYP71A9* (*Bs.00g241110.m01*) were induced by fluroxypyr treatment, as well as four Glutathione s-transferases (GSTs) in Flur-R at 3 and 10 HAT compared to the untreated timepoint.

When the downregulated 3 and 10 HAT timepoints were contrasted with the untreated timepoint within each line, Flur-R, J01-S, and 9425 identified 104 and 718 common fluroxypyr downregulated genes for the 3 and 10 HAT vs untreated timepoints, respectively (Figure 7C and D). Twelve of these shared genes were related to photosystem I and II at 10 HAT. Transcripts encoding key proteins related to photosynthetic electron transport such as Chlorophyll A-B binding protein (*Bs.00g240870.m01, Bs.00g240870.m02*) and ATP synthase (*Bs.00g432500.m01*) were downregulated in all three lines and were present in the top 20 downregulated genes for all three lines (Tables 6, 7, 8). Two chlorophyll biosynthesis regulator genes encoding Early light induced protein-1 (*Bs.00g421070.m01, Bs.00g420960.m01*) were uniquely downregulated and among the genes with the highest downregulation in both susceptible lines. These proteins play a role in preventing oxidative stress and excess accumulation of free chlorophyll (Hutin et al. 2003). Additionally, four Cellulose synthase genes (*Bs.00g015170.m01, Bs.00g015170.m02, Bs.00g056700.m01, Bs.00g260720.m01*) were downregulated in both susceptible lines and are of interest due to the role cellulose plays in cell wall structural support. Genes uniquely downregulated at 10 HAT in Flur-R included two additional photosystem II subunit genes (*Bs.00g059220.m01, Bs.00g338570.m01*) as well as genes encoding several synthases such as Terpene synthase (*Bs.00g074880.m01*), Polyprenyl synthetase (*Bs.00g449610.m01*), Strictosidine synthase (*Bs.00g057800.m01*), Phosphomethylpyrimidine synthase (*Bs.00g253210.m01*), Aminodeoxychorismate (ADC) synthase (*Bs.00g135570.m01*), and ABA biosynthesis gene *NCED2* (*Bs.00g024060.m01*).

3.6 Variant Analysis

Our decision criteria to determine resistance-conferring sequence variant candidates were that all four Flur-R individuals from the RNA-seq experiment must have the variant. The

candidate variant also must be absent in the two S lines (9425 and J01-S). Of the 147 genes annotated as CYP450s in the kochia genome, there were no unique variants in the Flur-R line. There were 37 genes annotated as having an Aux/IAA domain or function, and 21 genes with an ARF domain or function. Of these genes, three genes contained a nonsynonymous mutation or a deletion. ARF19/7 (*Bs.00g057730.m01*), one of five transcriptional activators in the ARF family, had two nonsynonymous mutations (Gly446Ser; Leu486Ile) and two single codon deletions (SI Figure 3A). A protein annotated as ARF3 (*Bs.00g076170.m01*) also known as ETTIN (ETT) showed one nonsynonymous homozygous variant (Leu293Ser), where three J01-S individuals were heterozygous for the variant found in Flur-R, one was homozygous, and the remaining four 9425 were wildtype. *Aux/IAA4-like* (*Bs.00g107340.m01*) displayed one nonsynonymous variant (Glu52Arg) in a non-conserved region 6-10 bases N terminal of the Aux/IAA Domain II described by Ramos et al. (2001) (SI Figure 3B). We also determined there were no variants in any proteins annotated as AFB or TIR1 proteins that were unique to Flur-R and met our specified criteria, and there were no mutations in the 18 LRR rich C terminus where Aux/IAA and auxin are reported to bind (Villalobos et al. 2012).

4. Discussion and Conclusion

Both fluroxypyr resistant line Flur-R and two susceptible lines 9425 and J01-S had up-regulation of auxin regulated genes in response to fluroxypyr that was similar to the auxin mimic herbicide gene expression response in Arabidopsis (Gleason et al. 2011; Goda et al. 2004). The increased expression of auxin responsive genes following fluroxypyr treatment suggests that fluroxypyr is being perceived similarly by all three lines and supports our findings that target-site variants found in *Aux/IAA4* and *ARF19/7* are likely not the cause of the fluroxypyr resistance response in Flur-R. Specifically in *ARF19/7*, the identified variants are predicted to have no significant effect on fluroxypyr binding due to their position in the variable middle region described by Ulmasov et al. (1999) (SI Figure 3A). Although we did find a Flur-R homozygous variant in *ARF3*, the region boundaries of *ARF3* are unlike most other ARFs in that it does not contain Domain III/IV, two key domains for interaction with Aux/IAA proteins relating to auxin gene expression. ARF3 does function in some auxin related pathways (reviewed by Liu et al. (2014)) but the protein has been described to function as a repressor of several proteins causing inhibition of cytokinin activity, a plant hormone that often partners with IAA (Zhang et al. 2018).

While we cannot be certain that the variant in *ARF3* does not contribute indirectly to fluroxypyr resistance or affect cytokinin levels in the plant, due to the ARF3 described function, there is stronger support for metabolism being the underlying cause of resistance. Additionally, if variants were found that affected auxin-mimic perception or binding, such as the *IAA16* Gly127Asn mutation described by LeClere et al. (2018), the expected auxin-response gene expression would likely not be induced as reported by Pettinga et al. (2018) in the 9425 line when tested with the auxin-mimic herbicide dicamba.

The translocation data suggest that fluroxypyr, being primarily in its acid form based on the 6 h metabolism results, is moving symplastically throughout the plant as a phloem mobile herbicide (Schober et al. 1986). Transcripts for two IAA transporter (PIN) isoforms were upregulated in the susceptible lines 9425 and J01-S when treated with fluroxypyr, suggesting that PINs can transport fluroxypyr in a similar manner to the transport of IAA. Based on the lack of differences in translocation between Flur-R and J01-S, these two identified PIN transporters are not moving phytotoxic fluroxypyr acid throughout the resistant or susceptible plants at a different rate. Other transporters such as ATP binding cassettes (ABCs) in class B can move multiple substrates including xenobiotics. Some members of this large protein family serve as auxin transporters (Cho and Cho 2013). ABC transporters from both class B and G were upregulated in Flur-R following fluroxypyr treatment, none of which have been individually implicated in herbicide resistance. Several class G transporters are involved in auxin homeostasis and other phytohormone transport, cellular detoxification of heavy metals, and pathogen resistance (Dhara and Raichaudhuri 2021; Gräfe and Schmitt 2021). The functional suite of ABC class G transporters in kochia is yet to be fully described, though cellular export of fluroxypyr conjugates is not outside the scope of known activity for class G transporters.

In Flur-R, abscisic acid (ABA) biosynthesis gene *NCED2* transcript expression decreased over a 10 h time period, contrasting the results from the two susceptible lines in which *NCED6* transcripts had increased expression at 3 h in all three lines (Figure 8). The implications of decreased *NCED2* expression in the resistant line are currently unknown, though some reports show an increased level of response from *NCED* genes following various auxin-mimic applications (Kraft et al. 2007; McCauley et al. 2020; Raghavan et al. 2005). Among these ABA related downregulated genes, seven subunits of Photosystem I and four subunits of Photosystem II are downregulated in all three lines following fluroxypyr application suggesting that

fluroxypyr may affect light energy harvesting as part of its mechanism of action. These findings are consistent with the findings of McCauley et al. (2020).

Of the five CYP450s constitutively expressed in Flur-R compared to either 9425 or J01-S, *CYP71D10/11* has been implicated in metabolic herbicide resistance to fenoxaprop-p-ethyl (Bai et al. 2020). Other CYP450s in the CYP71 family have been described as shikimate and shikimate intermediate modifiers (Jun et al. 2015), including Ent-kaurene oxidase (CYP701 subfamily) which functions in gibberellin biosynthesis; its overexpression causes partial resistance to plant growth retardant uniconazole-P (Miyazaki et al. 2011). *CYP81B2* (*Bs.00g431990.m01*) in transgenic tobacco metabolized the phenylurea herbicide chlortoluron after the application of auxin-mimic 2,4-D. The same study also identified its involvement in secondary metabolite biosynthesis (Ohkawa et al. 1999). The other two treatment induced CYP450s in Flur-R, *CYP82D47* and *CYP71A9-like*, have no described role in herbicide resistance, however, there are a significant number of CYP450s involved in herbicide metabolism in the CYP71 family, to which they both belong (Gion et al. 2014; Siminszky et al. 1999; Xiang et al. 2006).

The final constitutively expressed CYP450 in the Flur-R line, *CYP90C1/D1*, belongs to the CYP85 family which is implicated in modification of cyclic terpenes and sterols in brassinosteroid, abscisic acid and gibberellin biosynthesis (Jun et al. 2015; Ohnishi et al. 2006; Ohnishi et al. 2012). It is not unusual for CYP450s to be multifunctional (Bernhardt 2006), and their function can often be attributed to the selectivity of some herbicides, extensively reviewed by Dimaano and Iwakami (2021).

We investigated fluroxypyr resistance using herbicide physiology experiments as well as RNA-sequencing and identified metabolic detoxification as a plausible explanation of fluroxypyr resistance in kochia line Flur-R. Two of the four metabolites are accounted for, having been reported by the Environmental Protection Agency (EPA 2010). The action of conjugation by GSTs or GTs may explain one of the two remaining undescribed metabolites presented, which were both rapidly converted from fluroxypyr acid throughout the time course in Flur-R. Given the high expression of five GSTs and eight GTs in both untreated and treatment induced conditions, formation of secondary metabolic structures is possible. Following CYP450 activity via *O*-glucosylation, fluroxypyr-tripeptide GST or -sugar conjugates can be catalyzed by GST or UDP-glucosyl transferase (Ludwig-Müller 2011). GSTs and GTs can glycosylate plant hormones

and xenobiotics to influence bioactivity, transport, solubility and can be pumped out of the cell via ABC transporters (Li et al. 2001; Moons 2005). Subsequent sequestration of the non-phytotoxic herbicide via ABC transporter may also play a role in the resistance response in Flur-R, though more work is needed to fully understand the metabolic response following fluroxypyr application in Flur-R.

5. Future Work

Future work elucidating the fluroxypyr resistance mechanism involves *in vitro* and *in vivo* testing of the five candidate GSTs, eight GTs, and eight CYP450s. Metabolite identification via LCMS/MS is crucial next step to determine the metabolic path of the fluroxypyr molecule. Other future studies include genetic mapping of fluroxypyr resistance via test crosses and either Quantitative Trail Loci (QTL) or bulk-segregant analysis with resistant Flur-R and susceptible J01-S, which will provide chromosomal location of resistance gene(s) (Montgomery et al. 2023). Biochemical studies using P450 and GST inhibitors will indicate whether the enhanced fluroxypyr metabolism can be reversed. Metabolic information paired with mapping and ongoing inheritance studies will be a strong contribution to the understanding of auxin-mimic resistance and characterization of fluroxypyr resistance in this population of kochia. Identifying causal resistance genes in auxin-mimic resistant kochia populations will allow us to document the evolution of new resistance genes and predict patterns of gene flow, following the model set by Ravet et al. (2021) for gene flow of glyphosate resistance in kochia.

Data Availability:

The data underlying this article are available in the Gene Expression Omnibus at https://www.ncbi.nlm.nih.gov/geo/query/acc.cgi?acc=GSE179578, and can be accessed with GEO Accession GSE179578.

Author Contributions Using CRediT Author Statements

OT: Writing, visualization, data curation, investigation, formal analysis, validation, methodology **EP:** Resources, methodology **EW:** Resources **AA:** Investigation **WK:**

Investigation **FD:** Methodology, supervision, resources **SN:** Methodology, resources **TG:** Writing, supervision, conceptualization.

Acknowledgements

This research was supported in part by the Colorado Wheat Administrative Committee, by Corteva Agrisciences, and by the USDA National Institute of Food and Agriculture, Hatch project COL00783 to the Colorado State University Agricultural Experiment Station.

References

Aboul-Maaty N. A.-F., and H. A.-S. Oraby. (2019) Extraction of high-quality genomic DNA from different plant orders applying a modified CTAB-based method. Bulletin of the National Research Centre 43:25.

Bai S., Y. Zhao, Y. Zhou, M. Wang, Y. Li, X. Luo, and L. Li. (2020) Identification and expression of main genes involved in non-target site resistance mechanisms to fenoxaprop-p-ethyl in *Beckmannia syzigachne*. Pest Manag Sci 76:2619-2626.

Bernhardt R. (2006) Cytochromes P450 as versatile biocatalysts. J Biotechnol 124:128-45.

Busi R., D. E. Goggin, I. M. Heap, M. J. Horak, M. Jugulam, R. A. Masters, R. M. Napier, D. S. Riar, N. M. Satchivi, J. Torra, P. Westra, and T. R. Wright. (2018) Weed resistance to synthetic auxin herbicides. Pest Manag Sci 74:2265-2276.

Cho M., and H. T. Cho. (2013) The function of ABCB transporters in auxin transport. Plant Signal Behav 8:e22990.

Cingolani P., A. Platts, L. L. Wang, M. Coon, T. Nguyen, L. Wang, S. J. Land, X. Lu, and D. M. Ruden. (2012) A program for annotating and predicting the effects of single nucleotide polymorphisms, SnpEff: SNPs in the genome of Drosophila melanogaster strain w1118; iso-2; iso-3. Fly 6:80-92.

Delye C. (2013) Unravelling the genetic bases of non-target-site-based resistance (NTSR) to herbicides: a major challenge for weed science in the forthcoming decade. Pest Manag Sci 69:176-187.

Dhara A., and A. Raichaudhuri. (2021) ABCG transporter proteins with beneficial activity on plants. Phytochemistry 184:112663.

Dimaano N. G., and S. Iwakami. (2021) Cytochrome P450-mediated herbicide metabolism in plants: current understanding and prospects. Pest Manag Sci 77:22-32.

EPA. (2010) Analytical method for fluroxypyr-MHE and and its metabolites, fluroxypyr acid, fluroxypyr-DCP and fluroxypyr-MP in water. Available at epa.gov.

Figueiredo M. R., H. Barnes, C. M. Boot, A. B. T. De Figueiredo, S. J. Nissen, F. E. Dayan, and T. A. Gaines. (2022a) Identification of a novel 2, 4-D metabolic detoxification pathway in 2, 4-D-resistant waterhemp (*Amaranthus tuberculatus*). J Agr Food Chem 70:15380-15389.

Figueiredo M. R. A., L. J. Leibhart, Z. J. Reicher, P. J. Tranel, S. J. Nissen, P. Westra, M. L. Bernards, G. R. Kruger, T. A. Gaines, and M. Jugulam. (2018) Metabolism of 2,4-dichlorophenoxyacetic acid contributes to resistance in a common waterhemp (*Amaranthus tuberculatus*) population. Pest Manag Sci 74:2356-2362.

Figueiredo M. R. d., A. Küpper, J. M. Malone, T. Petrovic, A. B. T. d. Figueiredo, G. Campagnola, O. B. Peersen, K. V. Prasad, E. L. Patterson, and A. S. Reddy. (2022b) An in-frame deletion mutation in the degron tail of auxin coreceptor IAA2 confers resistance to the herbicide 2, 4-D in *Sisymbrium orientale*. Proc Natl Acad Sci USA 119:e2105819119.

Gaines T. A., S. O. Duke, S. Morran, C. A. G. Rigon, P. J. Tranel, A. Kupper, and F. E. Dayan. (2020) Mechanisms of evolved herbicide resistance. J Biol Chem 295:10307-10330.

Geddes C. M., M. L. Owen, T. E. Ostendorf, J. Y. Leeson, S. M. Sharpe, S. W. Shirriff, and H. J. Beckie. (2021a) Herbicide diagnostics reveal multiple patterns of synthetic auxin resistance in kochia (*Bassia scoparia*). Weed Technol:1-28.

Geddes C. M., T. E. Ostendorf, M. L. Owen, J. Y. Leeson, S. M. Sharpe, S. W. Shirriff, and H. J. Beckie. (2021b) Fluroxypyr-resistant kochia [*Bassia scoparia* (L.) AJ Scott] confirmed in Alberta. Can J Plant Sci 102:437-441.

Geddes C. M., M. M. Pittman, L. M. Hall, A. K. Topinka, S. M. Sharpe, J. Y. Leeson, and H. J. Beckie. (2022) Increasing frequency of multiple herbicide-resistant kochia (*Bassia scoparia*) in Alberta. Can J Plant Sci.

Gion K., H. Inui, K. Takakuma, T. Yamada, Y. Kambara, S. Nakai, H. Fujiwara, T. Miyamura, H. Imaishi, and H. Ohkawa. (2014) Molecular mechanisms of herbicide-inducible gene expression of tobacco CYP71AH11 metabolizing the herbicide chlorotoluron. Pestic Biochem Phys 108:49-57.

Gleason C., R. C. Foley, and K. B. Singh. (2011) Mutant analysis in Arabidopsis provides insight into the molecular mode of action of the auxinic herbicide dicamba. Plos One 6:e17245.

Goda H., S. Sawa, T. Asami, S. Fujioka, Y. Shimada, and S. Yoshida. (2004) Comprehensive comparison of auxin-regulated and brassinosteroid-regulated genes in Arabidopsis. Plant Physiol 134:1555-73.

Goggin D. E., S. Bringans, J. Ito, and S. B. Powles. (2019) Plasma membrane receptor-like kinases and transporters are associated with 2,4-D resistance in wild radish. Ann Bot.

Gräfe K., and L. Schmitt. (2021) The ABC transporter G subfamily in *Arabidopsis thaliana*. J Exp Bot 72:92-106.

Grossmann K. (2010) Auxin herbicides: current status of mechanism and mode of action. Pest Manag Sci 66:113-20.

Guilfoyle T. J. (1999) Auxin-regulated genes and promoters. Biochemistry and molecular biology of plant hormones.

Hall N., J. Chen, C. A. Saski, P. Westra, T. A. Gaines, and E. Patterson. (2023) FHY3/FAR1 transposable elements generate adaptive genetic variation in the *Bassia scoparia* genome. bioRxiv:2023.05. 26.542497.

Heap I. M. (2021) International survey of herbicide resistant weeds.

Hutin C., L. Nussaume, N. Moise, I. Moya, K. Kloppstech, and M. Havaux. (2003) Early light-induced proteins protect Arabidopsis from photooxidative stress. Proc Natl Acad Sci USA 100:4921-6.

Jha P., V. Kumar, and C. A. Lim. (2015) Variable response of kochia [*Kochia scoparia* (L.) Schrad.] to auxinic herbicides dicamba and fluroxypyr in Montana. Can. J. Plant Sci. 95:965-972.

Jonathon Anderson P. J. B., Daniel Milroy, Peter Ruprecht, Thomas Hauser, and Howard Jay Siegel. (2017) Deploying RMACC Summit: an HPC resource for the rocky mountain region. PEARC17.

Jun X., X.-y. WANG, and W.-z. GUO. (2015) The cytochrome P450 superfamily: key players in plant development and defense. J of Int Agric 14:1673-1686.

Kim D., J. M. Paggi, C. Park, C. Bennett, and S. L. Salzberg. (2019) Graph-based genome alignment and genotyping with HISAT2 and HISAT-genotype. Nat Biotech 37:907-915.

Knezevic S. Z., J. C. Streibig, and C. Ritz. (2007) Utilizing R software package for dose-response studies: the concept and data analysis. Weed Technol 21:840-848.

Kniss A. R., J. D. Vassios, S. J. Nissen, and C. Ritz. (2011) Nonlinear regression analysis of herbicide absorption studies. Weed Sci 59:601-610.

Kraft M., R. Kuglitsch, J. Kwiatkowski, M. Frank, and K. Grossmann. (2007) Indole-3-acetic acid and auxin herbicides up-regulate 9-cis-epoxycarotenoid dioxygenase gene expression and abscisic acid accumulation in cleavers (*Galium aparine*): interaction with ethylene. J Exp Bot 58:1497-503.

Kumar V., R. S. Currie, P. Jha, and P. W. Stahlman. (2019a) First report of kochia (*Bassia scoparia*) with cross-resistance to dicamba and fluroxypyr in western Kansas. Weed Technol 33:335-341.

Kumar V., P. Jha, M. Jugulam, R. Yadav, and P. W. Stahlman. (2019b) Herbicide-resistant kochia (*Bassia scoparia*) in North America: a review. Weed Sci 67:4-15.

LeClere S., C. Wu, P. Westra, and R. D. Sammons. (2018) Cross-resistance to dicamba, 2,4-D, and fluroxypyr in *Kochia scoparia* is endowed by a mutation in an AUX/IAA gene. Proc Natl Acad Sci USA 115:E2911-E2920.

Lee S., S. Sundaram, L. Armitage, J. P. Evans, T. Hawkes, S. Kepinski, N. Ferro, and R. M. Napier. (2014) Defining binding efficiency and specificity of auxins for SCF(TIR1/AFB)-Aux/IAA co-receptor complex formation. ACS Chem Biol 9:673-82.

Li Y., S. Baldauf, E.-K. Lim, and D. J. Bowles. (2001) Phylogenetic analysis of the UDP-glycosyltransferase multigene family of Arabidopsis thaliana. J Biol Chem 276:4338-4343.

Liao, Y., G. K. Smyth, and W. Shi. (2014) featureCounts: an efficient general purpose program for assigning sequence reads to genomic features. Bioinformatics 30:923-930.

Liu X., T. T. Dinh, D. Li, B. Shi, Y. Li, X. Cao, L. Guo, Y. Pan, Y. Jiao, and X. Chen. (2014) AUXIN RESPONSE FACTOR 3 integrates the functions of AGAMOUS and APETALA 2 in floral meristem determinacy. Plant J 80:629-641.

Ludwig-Müller J. (2011) Auxin conjugates: their role for plant development and in the evolution of land plants. J Exp Bot 62:1757-1773.

McCauley C. L., S. A. M. McAdam, K. Bhide, J. Thimmapuram, J. A. Banks, and B. G. Young. (2020) Transcriptomics in *Erigeron canadensis* reveals rapid photosynthetic and hormonal responses to auxin herbicide application. J Exp Bot 71:3701-3709.

Miyazaki S., T. Katsumata, M. Natsume, and H. Kawaide. (2011) The CYP701B1 of *Physcomitrella patens* is an ent-kaurene oxidase that resists inhibition by uniconazole-P. Febs Lett 585:1879-83.

Montgomery J. S., S. Morran, D. R. MacGregor, J. S. McElroy, P. Neve, C. Neto, M. M. Vila-Aiub, M. V. Sandoval, A. I. Menéndez, J. M. Kreiner, L. Fan, A. L. Caicedo, P. J. Maughan, B. A. B. Martins, J. Mika, A. Collavo, J. Aldo Merotto, N. K. Subramanian, M. V. Bagavathiannan, L. Cutti, M. M. Islam, B. S. Gill, R. Cicchillo, R. Gast, N. Soni,

T. R. Wright, G. Zastrow-Hayes, G. May, J. M. Malone, D. Sehgal, S. S. Kaundun, R. P. Dale, B. J. Vorster, B. Peters, J. Lerchl, P. J. Tranel, R. Beffa, M. Jugulam, K. Fengler, V. Llaca, E. L. Patterson, and T. Gaines. (2023) The International Weed Genomics Consortium: Community resources for weed genomics research. bioRxiv:2023.07.19.549613.

Moons A. (2005) Regulatory and functional interactions of plant growth regulators and plant glutathione S-transferases (GSTs). Vitam Horm 72:155-202.

Murphy B. P., and P. J. Tranel. (2019) Target-site mutations conferring herbicide resistance. Plants 8.

Ohkawa H., H. Tsujii, and Y. Ohkawa. (1999) The use of cytochrome P450 genes to introduce herbicide tolerance in crops: a review. Pestic Sci 55:867-874.

Ohnishi T., A.-M. Szatmari, B. Watanabe, S. Fujita, S. Bancos, C. Koncz, M. Lafos, K. Shibata, T. Yokota, and K. Sakata. (2006) C-23 hydroxylation by Arabidopsis CYP90C1 and CYP90D1 reveals a novel shortcut in brassinosteroid biosynthesis. Plant Cell 18:3275-3288.

Ohnishi T., B. Godza, B. Watanabe, S. Fujioka, L. Hategan, K. Ide, K. Shibata, T. Yokota, M. Szekeres, and M. Mizutani. (2012) CYP90A1/CPD, a brassinosteroid biosynthetic cytochrome P450 of Arabidopsis, catalyzes C-3 oxidation. J Biol Chem 287:31551-31560.

Paponov I. A., M. Paponov, W. Teale, M. Menges, S. Chakrabortee, J. A. Murray, and K. Palme. (2008) Comprehensive transcriptome analysis of auxin responses in Arabidopsis. Mol Plant 1:321-37.

Perrot-Rechenmann C. (2010) Cellular responses to auxin: division versus expansion. Cold Spring Harb Perspect Biol 2:a001446.

Pettinga D. J., J. Ou, E. L. Patterson, M. Jugulam, P. Westra, and T. A. Gaines. (2018) Increased chalcone synthase (CHS) expression is associated with dicamba resistance in *Kochia scoparia*. Pest Manag Sci 74:2306-2315.

Preston C., D. S. Belles, P. H. Westra, S. J. Nissen, and S. M. Ward. (2009) Inheritance of resistance to the auxinic herbicide dicamba in kochia (*Kochia scoparia*). Weed Sci 57:43-47.

R Core Team (2020). R: A language and environment for statistical computing. R Foundation for Statistical Computing, Vienna, Austria. URL http://www.R-project/org/.

Raghavan C., E. K. Ong, M. J. Dalling, and T. W. Stevenson. (2005) Effect of herbicidal application of 2,4-dichlorophenoxyacetic acid in Arabidopsis. Funct Integr Genomics 5:4-17.

Ramos J. A., N. Zenser, O. Leyser, and J. Callis. (2001) Rapid degradation of auxin/indoleacetic acid proteins requires conserved amino acids of domain II and is proteasome dependent. Plant Cell 13:2349-2360.

Ravet K., C. D. Sparks, A. L. Dixon, A. Küpper, E. P. Westra, D. J. Pettinga, P. J. Tranel, J. Felix, D. W. Morishita, and P. Jha. (2021) Genomic-based epidemiology reveals independent origins and gene flow of glyphosate resistance in *Bassia scoparia* populations across North America. Mol Ecol 30:5343-5359.

Rimmer A., H. Phan, I. Mathieson, Z. Iqbal, S. R. Twigg, A. O. Wilkie, G. McVean, and G. Lunter. (2014) Integrating mapping-, assembly-and haplotype-based approaches for calling variants in clinical sequencing applications. Nat Genet 46:912-918.

Robinson J. T., H. Thorvaldsdóttir, A. M. Wenger, A. Zehir, and J. P. Mesirov. (2017) Variant review with the integrative genomics viewer. Cancer Res 77:e31-e34.

Rosquete M. R., E. Barbez, and J. Kleine-Vehn. (2012) Cellular auxin homeostasis: gatekeeping is housekeeping. Mol Plant 5:772-86.

Schober A., S. McMaster, and R. Gantz. (1986) Fluroxypyr: a new environmentally compatible herbicide Proceedings-Western Society of Weed Science (USA).

Siminszky B., F. T. Corbin, E. R. Ward, T. J. Fleischmann, and R. E. Dewey. (1999) Expression of a soybean cytochrome P450 monooxygenase cDNA in yeast and tobacco enhances the metabolism of phenylurea herbicides. Proc Natl Acad Sci USA 96:1750-1755.

Teale W. D., I. A. Paponov, and K. Palme. (2006) Auxin in action: signalling, transport and the control of plant growth and development. Nat Rev Mol Cell Biol 7:847-59.

Todd O. E., M. R. Figueiredo, S. Morran, N. Soni, C. Preston, M. F. Kubeš, R. Napier, and T. A. Gaines. (2020) Synthetic auxin herbicides: finding the lock and key to weed resistance. Plant Sci 300:110631.

Tranel P. J., and T. R. Wright. (2002) Resistance of weeds to ALS-inhibiting herbicides: what have we learned? Weed Sci 50:700-712.

Ulmasov T., G. Hagen, and T. J. Guilfoyle. (1999) Activation and repression of transcription by auxin-response factors. Proc Natl Acad Sci USA 96:5844-5849.

Varanasi V. K., A. S. Godar, R. S. Currie, A. J. Dille, C. R. Thompson, P. W. Stahlman, and M. Jugulam. (2015) Field-evolved resistance to four modes of action of herbicides in a single kochia (*Kochia scoparia* L. Schrad.) population. Pest Manag Sci 71:1207-12.

Villalobos L. I. A. C., S. Lee, C. De Oliveira, A. Ivetac, W. Brandt, L. Armitage, L. B. Sheard, X. Tan, G. Parry, H. B. Mao, N. Zheng, R. Napier, S. Kepinski, and M. Estelle. (2012) A combinatorial TIR1/AFB-Aux/IAA co-receptor system for differential sensing of auxin. Nat Chem Biol 8:477-485.

Westra E. P., S. J. Nissen, T. J. Getts, P. Westra, and T. A. Gaines. (2019) Survey reveals frequency of multiple resistance to glyphosate and dicamba in kochia (*Bassia scoparia*). Weed Technol 33:664-672.

Wu C., S. LeClere, K. Liu, M. Paciorek, A. Perez-Jones, P. Westra, and R. D. Sammons. (2020) A dicamba resistance-endowing IAA16 mutation leads to significant vegetative growth defects and impaired competitiveness in kochia (*Bassia scoparia*). Pest Manag Sci 77:795-804.

Xiang W. S., X. J. Wang, and T. R. Ren. (2006) Expression of a wheat cytochrome P450 monooxygenase cDNA in yeast catalyzes the metabolism of sulfonylurea herbicides. Pestic Biochem Phys 85:1-6.

Xu J., X. Liu, R. Napier, L. Dong, and J. Li. (2022) Mode of action of a novel synthetic auxin herbicide halauxifen-methyl. Agronomy 12:1659.

Zhang K., R. Wang, H. Zi, Y. Li, X. Cao, D. Li, L. Guo, J. Tong, Y. Pan, and Y. Jiao. (2018) AUXIN RESPONSE FACTOR3 regulates floral meristem determinacy by repressing cytokinin biosynthesis and signaling. Plant Cell 30:324-346.

Zhao Y. (2010) Auxin biosynthesis and its role in plant development. Annu Rev Plant Biol 61:49-64.

FIGURES

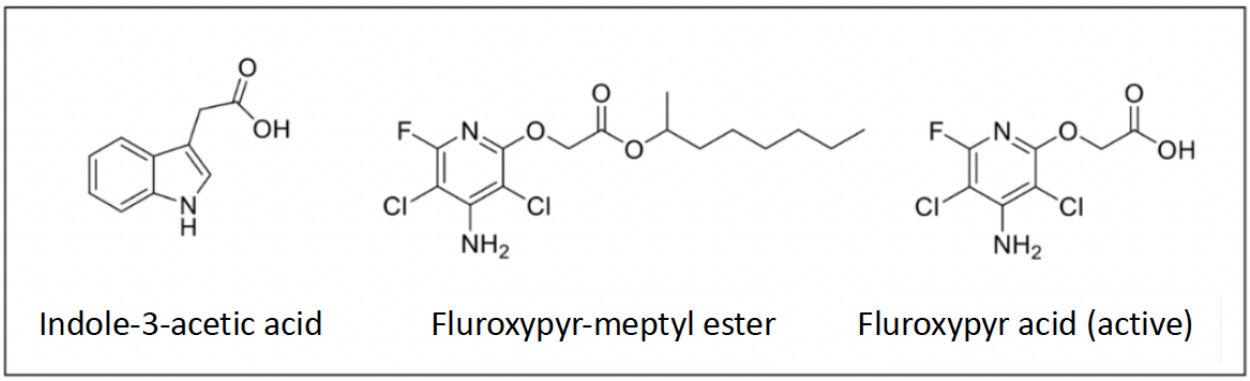

Figure 1: Chemical structure of indole-3-acetic acid (IAA), fluroxypyr-meptyl ester (fluroxypyr-ester) included in the formulated commercial products, and fluroxypyr-acid, the biologically active form of the herbicide. Deesterification of fluroxypyr-meptyl ester frees the carboxyl group shown in fluroxypyr-acid, which plays a key role in plant perception related to the auxin signaling pathway in relation to the ring structure found throughout auxin-mimic herbicide chemistry.

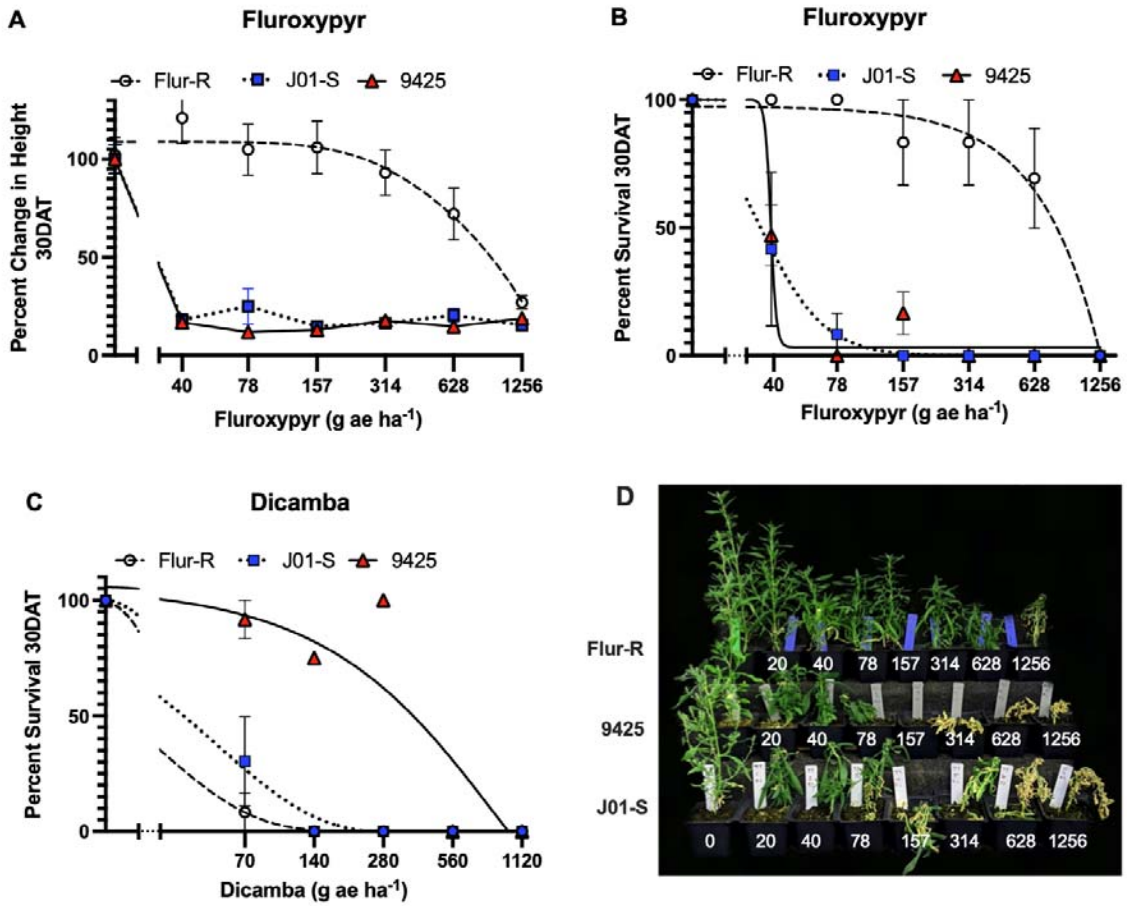

Figure 2: Dose response data for (A, B) fluroxypyr (no adjuvant) and (C) dicamba (+ 0.25% NIS) demonstrated fluroxypyr resistance and dicamba sensitivity in fluroxypyr resistant line Flur-R. X-axis is represented in a log10 scale. A. Percent change in height as a percent of the untreated control 30 days after treatment with fluroxypyr showed a 25% reduction in height in Flur-R at 628 g ae ha^{-1} (four times the label rate of 157 g ae ha^{-1}). B. Percent survival for Flur-R with greater than 70% survival to fluroxypyr at 628 g ae ha^{-1} (LD_{50} = 720, p= <0.001). The population 9425 was susceptible to fluroxypyr (LD_{50} = 20 g ae ha^{-1}, p <0.001). C. Flur-R was susceptible to dicamba (LD_{50} = 56 g ae ha^{-1}, p <0.001) and the known dicamba-resistant line, 9425, was resistant to dicamba up to 280 g ae ha^{-1}. Error bars represent SEM. D. Singular plants represent the average line response at each dose of fluroxypyr where 157 g ae ha^{-1} represents the label rate.

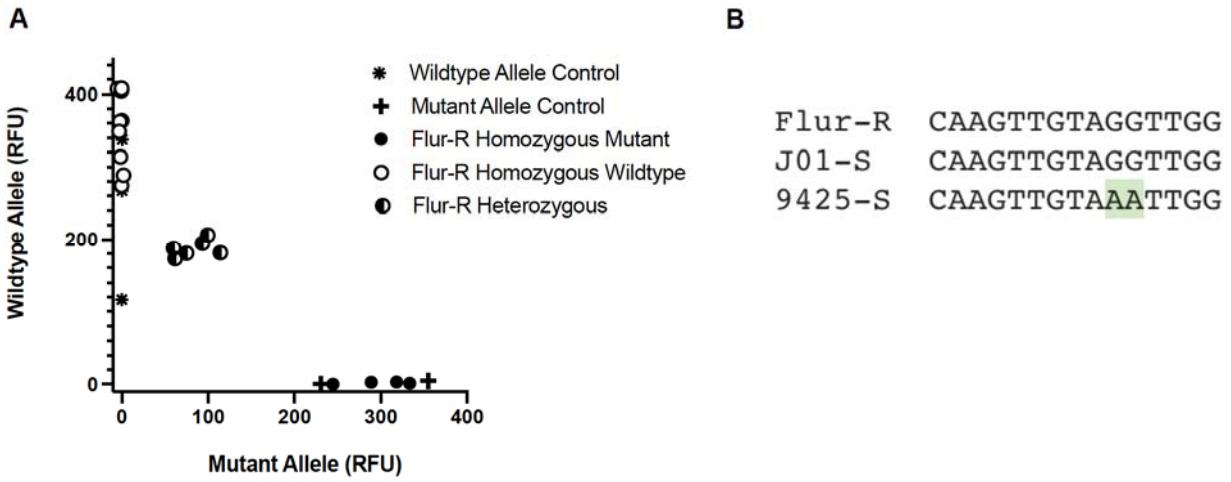

Figure 3: A. KASP assay with fluroxypyr resistant individuals sprayed with 157 g ai ha^{-1} fluroxypyr. Wildtype allele control lines were fluroxypyr and dicamba susceptible line 7710 and J01-S. Mutant allele control was homozygous dicamba resistant line 9425. B. Consensus sequenced based on KASP and previously published sequencing data at the mutation point of interest in J01-S, Flur-R and dicamba resistant line 9425 conferring resistance to dicamba as reported by LeClere et al. 2018. The mutation from GG to AA confers a G127N change.

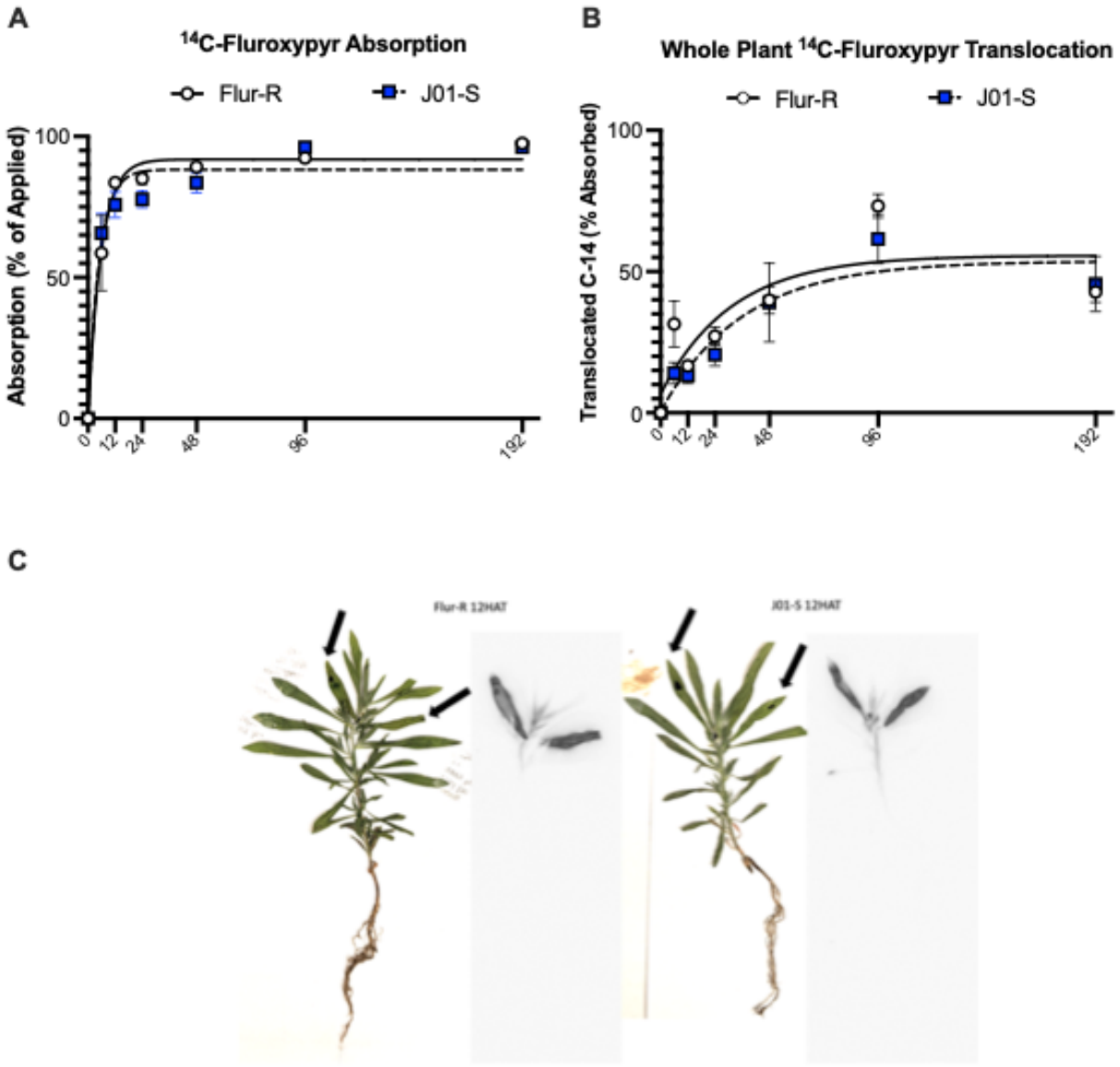

Figure 4. Whole plant absorption (A) and translocation (B) of fluroxypyr on resistant Flur-R line and susceptible line J01-S assessed over 6, 12, 24, 48, 96, and 192 h after treatment with [^{14}C]-fluroxypyr ester. The absorption and translocation graphs depict mean percent absorption as percent of applied radiation and mean percent translocation as percent of absorbed radiation to account for slight variation in application rates, with error bars representing SEM. There were no differences in absorption or translocation of [^{14}C]-fluroxypyr ester between Flur-R and J01-S. C. Pressed plant and phosphor-images showed translocation of [^{14}C]-fluroxypyr ester in Flur-R (left) and J01-S (right) at 12 h, the time at which max absorption was at 90% in both lines. The black arrows mark the two treated meristem leaves on each individual. The phosphor image to the right of each pressed plant photo shows early-stage translocation of [^{14}C]-fluroxypyr ester.

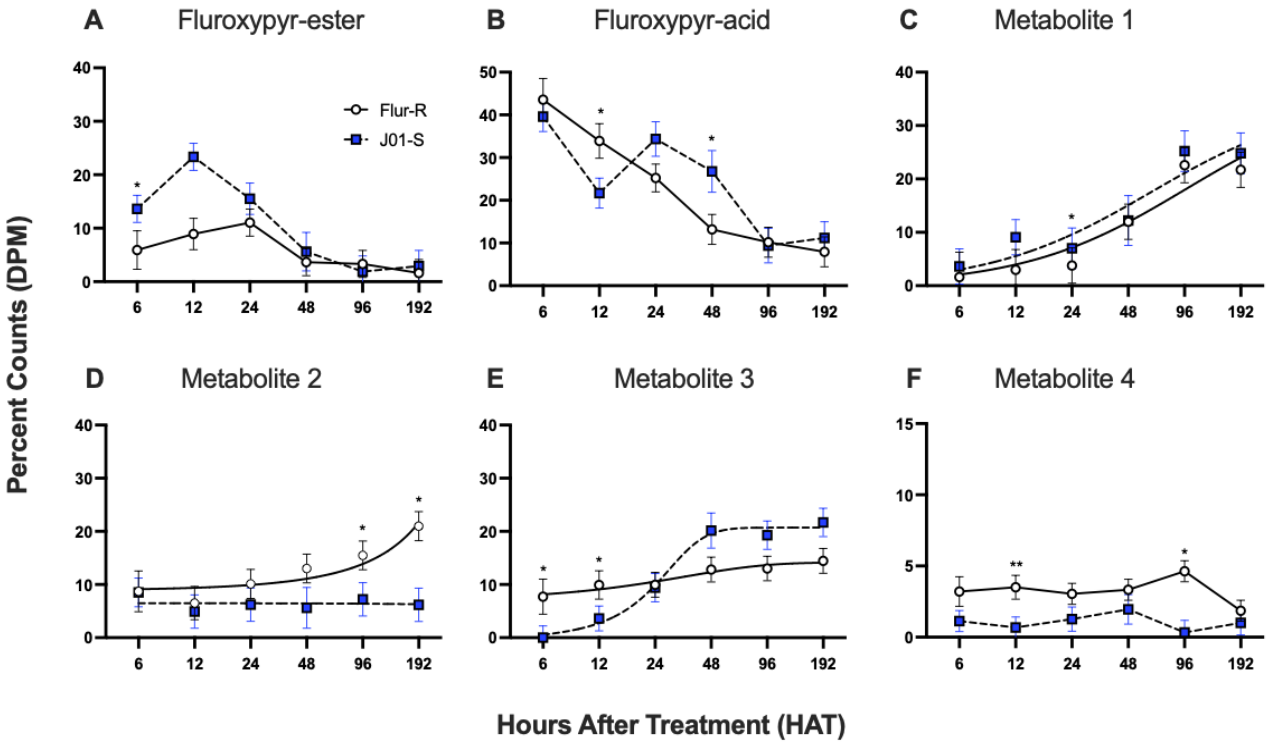

Figure 5. HPLC fluroxypyr parent and metabolite profiles over a 192 h time-course in fluroxypyr resistant kochia (*Bassia scoparia)* line Flur-R and fluroxypyr susceptible J01-S. A. Parent compound, [^{14}C]-fluroxypyr ester (9.5 min retention). B. Biologically active compound, [^{14}C]-fluroxypyr acid (7.7 min retention). C. Unknown metabolite 1 (4.5 min retention). D. Unknown metabolite 2 (5.8 min retention). E. Unknown metabolite 3 (6.4 min retention). F. Unknown metabolite 4 (7.2 min retention). * $P<0.05$, ** $P\leq0.005$, error bars represent SEM.

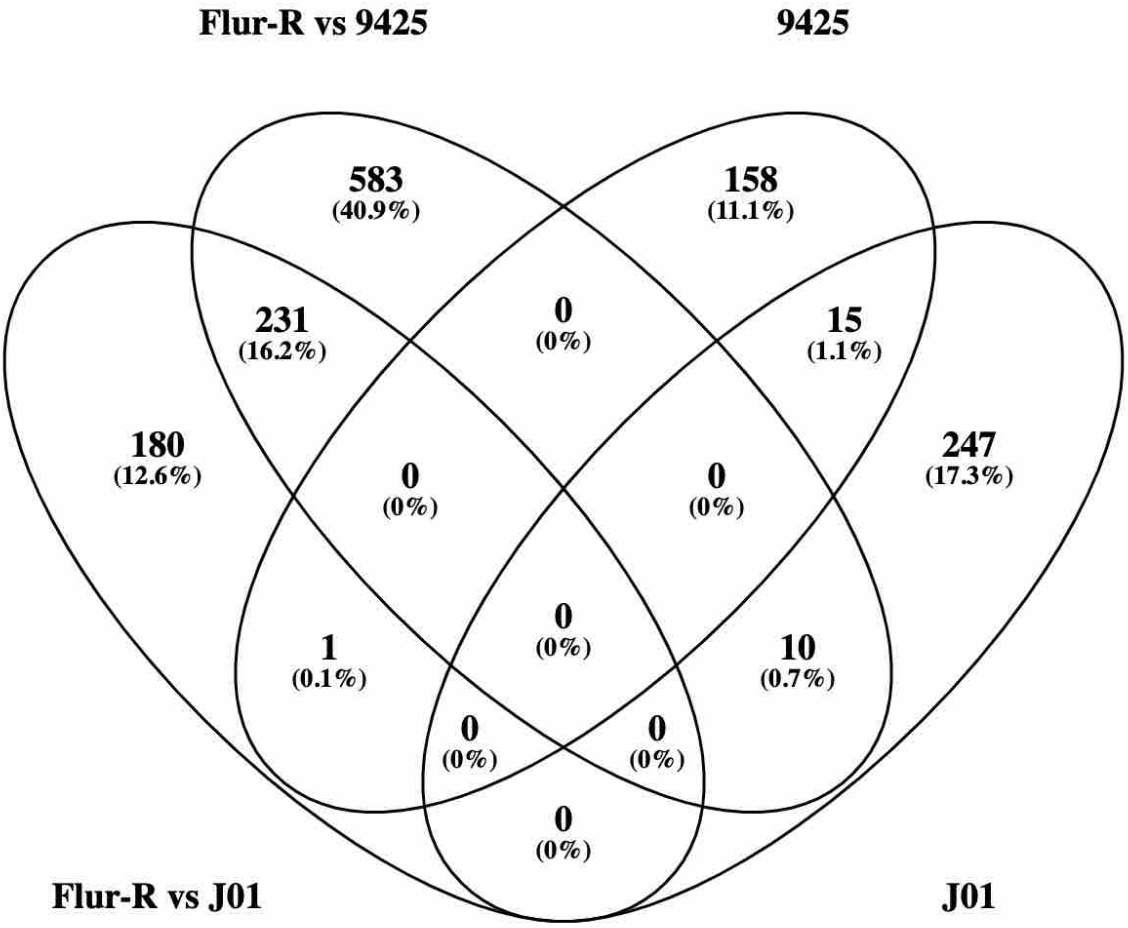

Figure 6. Venn diagram of upregulated genes between the untreated condition in Flur-R compared to both untreated conditions in fluroxypyr susceptible lines 9425-S and J01-S in DESeq2 (Flur-R vs 9425; Flur-R vs J01). Genes upregulated in both 9425-S and J01-S compared to Flur-R in DESeq2 are represented by their singular line name in the diagram (J01, 9425). Overlapping ovals represent genes that are commonly expressed at the untreated condition between comparisons.

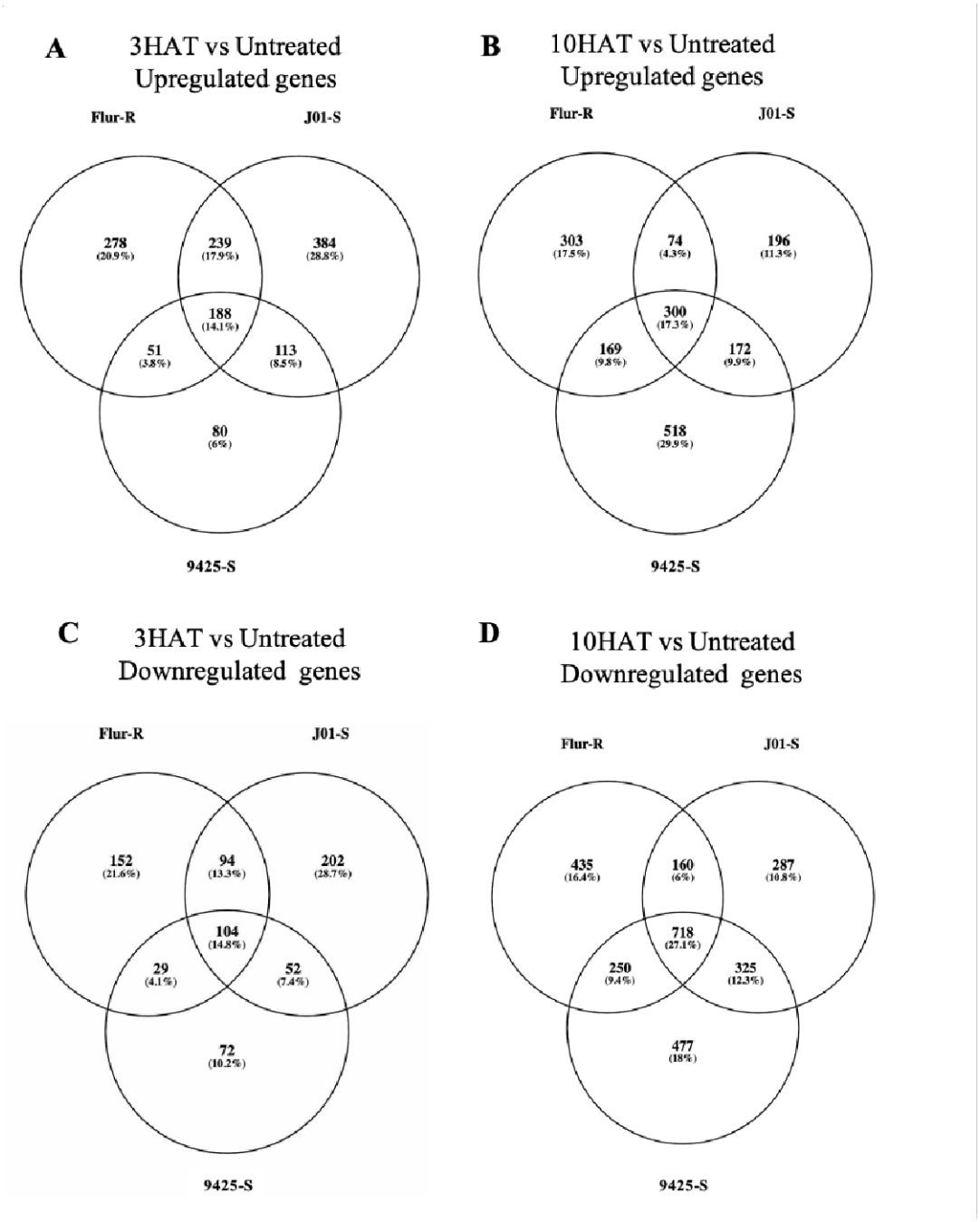

Figure 7. Number of transcripts that were either up or down regulated between the untreated condition and either 3 or 10 h after treatment (HAT) with fluroxypyr in fluroxypyr-resistant line Flur-R and susceptible lines 9425 and J01-S. A. Shared and uniquely upregulated genes at 3 HAT among and between all three lines. B. Shared and uniquely upregulated genes at 10 HAT among and between all three lines. C. Shared and uniquely downregulated genes at 3 HAT among and between all three lines. D. Shared and uniquely downregulated genes at 10 HAT among and between all three lines.

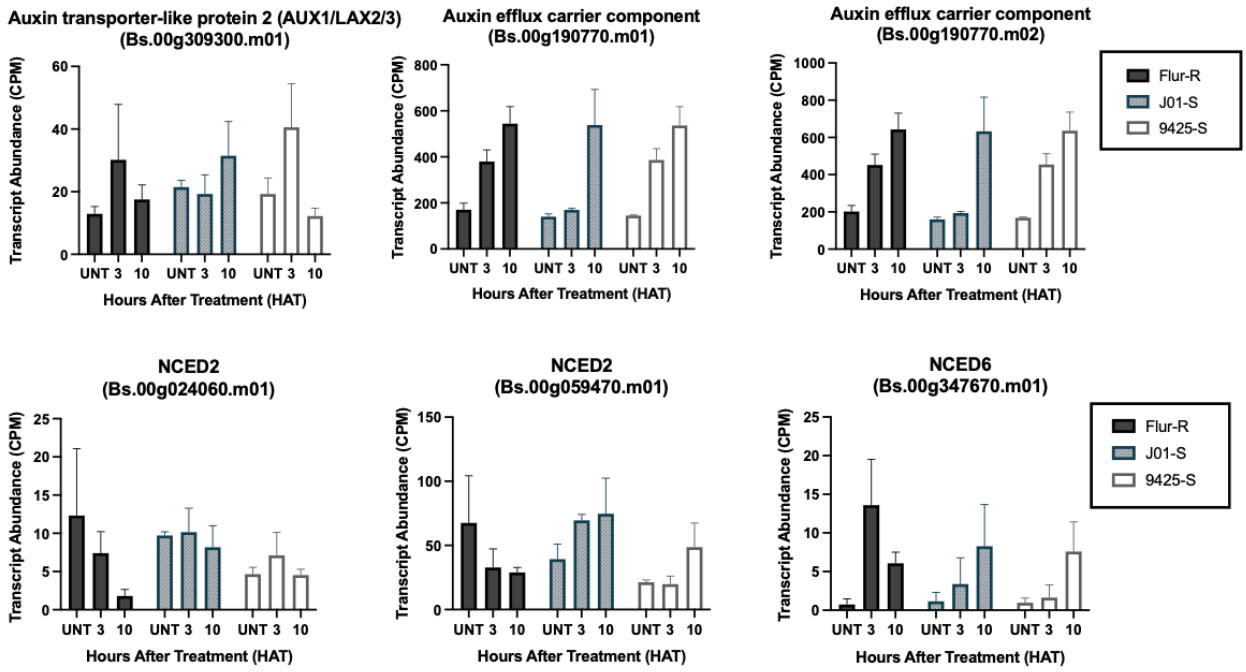

Figure 8. Expression profiles for auxin induced influx and efflux transporters and NCED in fluroxypyr-resistant kochia (*Bassia scoparia*) Flur-R, susceptible J01-S, and susceptible 9425 following differential expression analysis of RNA-Seq data. X-axis treatments: untreated, 3 h after treatment (HAT), and 10 HAT grouped by kochia line. Normalized counts on the y-axis were a result of the DESeq2 function and model fitting in R package "DESeq2". Both isoforms of the auxin efflux carrier component were upregulated in response to fluroxypyr in the 9425 line. There were no differences in expression for the Aux/LAX transporter. NCED6 was induced at both 3 HAT and 10 HAT in Flur-R, while NCED2 was downregulated in Flur-R.

TABLES

Table 1. Parameters for fluroxypyr dose-response data in kochia (*Bassia scoparia*) populations Flur-R, 9425, and J01-S. Parameters of the fluroxypyr and dicamba dose-responses for percent survival parameters are described in Equation 3 for Flur-R, fluroxypyr sensitive line J01-S and fluroxypyr sensitive/dicamba resistant line 9425. Flur-R shows a significant resistance factor ratio (R/S) of 36 and 40 relative to 9425 and J01, respectively. (*b*,*d*) Lower and upper limits of regression parameters, respectively. (*LD_{50}*) The dose (g ae ha^{-1}) of fluroxypyr where 50% mortality occurs for each population. (*R/S)* The ratio of resistant LD_{50} to either susceptible LD_{50} and associated p-values.

	Herbicide									
	Fluroxypyr					Dicamba				
Line	*b* (± SE)	*d* (± SE)	LD_{50} (± SE)	R/S	P-value	*b* (± SE)	*d* (± SE)	LD_{50} (± SE)	R/S	P-value
	-----g ae ha^{-1}-----					-----g ae ha^{-1}-----				
Flur-R	7.3 (8.4)	94.5 (3.6)	720 (110.3)	36-40	<0.001	7.4 (5.2)	100.0 (4.9)	56 (8.5)	--	--
9425	8.5 (37.7)	100.0 (8.8)	20 (1.5)	--	--	85.1 (10.0)	91.7 (2.72)	415 (10.0)	6-7	<0.001
J01-S	3.1 (1.8)	100.0 (8.8)	18 (2.7)	--	--	9.3 (8.5)	100.0 (4.93)	64 (5.4)	--	--

Table 2. Genes with higher expression at the untreated timepoint in kochia (*Bassia scoparia*) line Flur-R compared to 9425 and J01-S lines at the untreated timepoint. Raw normalized counts and Log2 fold change for highly expressed ABC transporters, UDP glucosyltransferases, and cytochrome P450 monooxygenases in the fluroxypyr-resistant population Flur-R compared to either susceptible population 9425 or J01-S. Genes which are higher expressed in Flur-R compared to both susceptible populations and are denoted with † and represented with the normalized count and fold change comparison to 9425. Log2 Fold Change was calculated in DESeq2, log2 fold change standard error and adjusted *p*-value were also calculated in DESeq2. The Wald-test obtained *p*-values were adjusted using the Benjamini-Hochberg method. The FDR was < 0.05.

Gene ID	Mean of normalized counts		Fold Change	Log2 Fold Change (±SE)	P-value (adjusted)	Gene Description
	Flur-R	9425				
Bs.00g184080.m02	2258	3	753	9.70 (0.75)	1.85E-32	ABC-G 34 Isoform 2
Bs.00g184080.m01	2147	3	716	9.63 (0.75)	9.86E-32	ABC-G 34 Isoform 1
Bs.00g217020.m01†	63	0	63	8.98 (2.85)	1.31E-06	ABC-G 31-like
Bs.00g142060.m01	38	0	38	8.02 (2.81)	6.52E-05	UDP-glucosyltransferase 73B2 related
Bs.00g184110.m01	133	2	67	6.24 (0.96)	3.59E-08	CYP701 subfamily (Ent- Kaurene Oxidase)
Bs.00g282300.m01†	108	6	18	5.18 (1.47)	0.0028	ABC-G 28-like
Bs.00g480980.m01†	510	14	36	5.01 (0.63)	2.11E-11	UDP-glucuronosyl/UDP-glucosyltransferase 89A2-like
Bs.00g480980.m03†	538	15	36	4.99 (0.63)	2.72E-11	UDP-glucuronosyl/UDP-glucosyltransferase 89A2-like
Bs.00g541440.m01	232	10	23	4.21 (0.72)	2.00E-06	CYP96A15
Bs.00g051830.m01	233	5	47	4.03 (1.48)	0.0231	CYP71D10/11
Bs.00g454440.m01†	276	52	5	2.28 (0.44)	0.0003	Putative ABC-B 28-like
Bs.00g061050.m01	6018	1187	5	2.08 (0.59)	0.027	UDP-glycosyltransferase 87A1 related
Bs.00g251290.m01	1462	341	4	1.98 (0.38)	0.0008	ABC-G 29-like
Bs.00g245700.m01	417	114	4	1.72 (0.40)	0.0113	CYP90C1/D1 (3-Epi-6-Deoxocathasterone 23-Monooxygenase)
	Flur-R	J01-S				
Bs.00g486870.m01	1847	61	31	4.85 (0.55)	1.29E-13	CYP82D47-like
Bs.00g142720.m01	8246	3606	2	1.17 (0.15)	0.0001	7-deoxyloganetin glucosyltransferase-like 85A23

Table 3. Top 20 upregulated genes in fluroxypyr-resistant kochia (*Bassia scoparia*) line Flur-R at 3 h after treatment (HAT) and 10 HAT compared to the untreated timepoint. Fold change was calculated using the mean of normalized counts, which was produced using the DESeq2 package in R. Log2 Fold Change was calculated in DESeq2, log2 fold change standard error and adjusted *p*-value were also calculated in DESeq2. The Wald-test obtained *p*-values were adjusted using the Benjamini-Hochberg method. The FDR was < 0.05.

Gene ID	Mean of normalized counts		Fold Change	Log2 Fold Change (±SE)	P-value	Gene Description
	Flur-R Untreated	Flur-R 3HAT				
Bs.00g016210.m01[j] †	0.71	607	855	5.30 (0.39)	1.59E-14	Precursor of CEP13/CEP14
Bs.00g306100.m01	8	383	48	4.79 (0.33)	2.84E-28	Transcription Factor, MADS-Box
Bs.00g477580.m01[c] †				4.63 (0.40)	1.22E-35	GH3 Family Protein
Bs.00g523550.m01	20	1131	57	4.57 (0.380	8.34E-24	Reverse Transcriptase Zinc-Binding Domain
Bs.00g418990.m01	34	1534	45	4.48 (0.37)	3.11E-23	Ethylene-Responsive Transcription Factor
Bs.00g010340.m01	1187	24154	20	4.43 (0.28)	3.94E-42	Membrane Attack Complex Component/Perforin (MACPF) Domain
Bs.00g435130.m01	34	1425	42	4.11 (0.39)	2.77E-19	Proton-Dependent Oligopeptide Transporter Family
Bs.00g315820.m01	242	7163	30	4.03 (0.37)	2.01E-18	Amino Acid Transporter
Bs.00g520970.m01	4	791	198	3.98 (0.47)	3.34E-13	Uncharacterized Protein
Bs.00g419000.m01[a]	4	1779	445	3.99 (0.49)	3.20E-11	Dehydration-Responsive Element-Binding Protein 1A-Related
Bs.00g315840.m01	184	5117	28	3.92 (0.38)	1.28E-16	Amino Acid Transporter
Bs.00g301780.m01	650	24203	37	3.90 (0.40)	2.28E-17	ABC Transporter G Family Member 40
Bs.00g087440.m01	17	547	32	3.88 (0.40)	5.86E-14	Amino Acid Transporter
Bs.00g181270.m02[a]	150	5353	36	3.87 (0.42)	4.17E-14	Protein NLP6-Related
Bs.00g257560.m01	1	330	330	3.85 (0.45)	3.93E-11	C2 Domain (Calcium/Lipid-Binding Domain, Calb)
Bs.00g200680.m01	1	80	80	3.85 (0.42)	2.58E-07	Uncharacterized Protein
Bs.00g244620.m01	75	1873	25	3.85 (0.34)	7.44E-20	Uncharacterized Protein
Bs.00g301770.m01	65	2253	35	3.82 (0.40)	3.74E-16	ABC Transporter G Family Member 40
Bs.00g428240.m01	3	126	42	3.78 (0.42)	3.22E-10	Extended Synaptotagmin-Related

Bs.00g036810.m01	750	16564	22	3.73 (0.36)	1.72E-17	Protein Phosphatase 2C
	Flur-R Untreated	Flur-R 10 HAT				
Bs.00g016210.m01[j] †	0.71	2485	4007	7.43 (0.36)	9.28E-23	Precursor of CEP13/CEP14
Bs.00g477580.m01[c] †	67	29708	443	6.01 (0.41)	6.01E-57	GH3
Bs.00g239120.m01[k]	7	1135	162	5.82 (0.39)	1.82E-33	Aquaporin Transporter
Bs.00g168520.m01[k]	35	3260	93	5.25 (0.35)	1.44E-36	Cold Regulated Protein 27
Bs.00g168520.m02[d]	37	3298	89	5.41 (0.38)	1.41E-43	Cold Regulated Protein 27
Bs.00g107600.m01	13	2990	230	5.21 (0.43)	7.35E-34	Barwin-like endoglucanases
Bs.00g370370.m01	3	495	65	5.14 (0.41)	1.50E-22	Ethylene-Responsive Transcription Factor 13 Related
Bs.00g431740.m01	33	4437	134	5.12 (0.44)	2.94E-27	Heme-Dependent Peroxidases
Bs.00g057300.m01	0.34	142	418	5.06 (0.49)	3.98E-08	CYP71D10-like
Bs.00g217150.m01	6	1485	248	4.92 (0.44)	4.39E-28	Bet v I/Major Latex Protein
Bs.00g122020.m01	42	16883	393	4.88 (033)	2.86E-36	Uncharacterized Protein
Bs.00g261130.m01	43	6160	143	4.83 (0.33)	1.71E-23	Bet v I/Major Latex Protein
Bs.00g291860.m01	0	153	153	4.78 (0.47)	7.06E-11	Secoisolariciresinol Dehydrogenase
Bs.00g478760.m01[h]	1	930	930	4.48 (0.46)	5.42E-19	1-Aminocyclopropane-1-Carboxylate Synthase 4 Related
Bs.00g282410.m01	6	730	122	4.43 (0.45)	2.22E-19	Cysteine-Rich Repeat Secretory Protein 38
Bs.00g056520.m01	532	16588	31	4.39 (0.33)	5.82E-31	Alanine Dehydrogenase/Pyridine Nucleotide Transhydrogenase
Bs.00g370420.m01	0.37	76	205	4.35 (0.45)	5.86E-07	Uncharacterized Protein
Bs.00g422990.m01[d]	4681	137203	29	4.28 (0.32)	4.34E-32	4-Hydroxyphenylpyruvate Dioxygenase-like
Bs.00g020740.m01	5	709	142	4.27 (0.48)	1.40E-16	WRKY Transcription Factor
Bs.00g148640.m01[m]	1158	32325	28	4.26 (0.30)	7.67E-36	2-Oxoisovalerate Dehydrogenase Subunit Alpha 2

[a] Shared between J01-S 3 HAT and Flur-R 3 HAT top 20 upregulated genes
[c] Shared between 9425-S 10 HAT, J01-S 10 HAT and Flur-R 3/10 HAT top 20 upregulated genes
[d] Shared between J01-S 10 HAT and Flur-R 3 HAT upregulated top 20 upregulated genes
[h] Shared between 9425-S 3 HAT, Flur-R 10 HAT and J01-S 10 HAT top 20 upregulated genes
[j] Shared between 9425-S 10 HAT, Flur-R 3 HAT /10 HAT and J02-S 10 HAT top 20 upregulated genes
[k] Shared between 9425-S 10 HAT, Flur-R 10 HAT and J01-S 10 HAT top 20 upregulated genes
[m] Shared between 9425-S 10 HAT and Flur-R 10 HAT top 20 upregulated genes

† Shared between Flur-R 3 HAT/10 HAT top 20 upregulated genes

Table 4. Top 20 upregulated genes in fluroxypyr-susceptible kochia (*Bassia scoparia*) line J01-S at 3 h after treatment (HAT) and 10 HAT compared to the untreated timepoint. Fold change was calculated using the mean of normalized counts which was produced using the DESeq2 package in R. Log2 Fold Change was calculated in DESeq2, log2 fold change standard error and adjusted *p*-value were also calculated in DESeq2. The Wald-test obtained *p*-values were adjusted using the Benjamini-Hochberg method. The FDR was <0.05.

Gene ID	Mean of normalized counts		Fold Change	Log2 Fold Change (±SE)	P-value	Gene Description
	J01-S Untreated	J01-S 3 HAT				
Bs.00g058350.m01	4	3428	763	7.33 (0.40)	2.01E-40	NADH Oxidoreductase-Related
Bs.00g144030.m01	173	40872	237	6.42 (0.44)	1.39E-37	Glycoside Hydrolase, Family 16
Bs.00g487370.m01	3	694	247	5.84 (0.46)	1.66E-17	Alpha/Beta Hydrolase Fold
Bs.00g397110.m01	0	494	494	5.46 (0.51)	1.71E-09	Zinc Finger, RING/FYVE/PHD-Type
Bs.00g435120.m01	31	2720	87	5.44 (0.37)	2.45E-36	Proton-Dependent Oligopeptide Transporter Family
Bs.00g419000.m01[a]	0	762	762	5.43 (0.53)	4.51E-10	AP2/ERF
Bs.00g122020.m01†	20	10546	515	5.43 (0.46)	4.17E-37	Uncharacterized Protein
Bs.00g142660.m01	232	13906	60	5.39 (0.32)	6.56E-47	Exordium-Like
Bs.00g430680.m01	5	8380	1847	5.38 (0.53)	2.75E-25	Protein Phosphatase 2C Family
Bs.00g167370.m01	23	2527	110	5.23 (0.48)	2.31E-18	Elo, Fatty Acid Acyl Transferase-Related
Bs.00g058830.m01	337	54400	162	5.20 (0.50)	5.41E-20	Harbinger Transposase-Derived Nuclease Domain
Bs.00g415260.m01	328	31294	95	5.12 (0.46)	4.78E-21	WRKY Domain
Bs.00g361960.m01	24	1628	67	4.96 (0.43)	1.07E-20	Gibberellin 2-Beta-Dioxygenase 4
Bs.00g428250.m02	34	5275	154	4.87 (0.52)	7.13E-16	C2 Domain (Calcium/Lipid-Binding Domain, Calb)
Bs.00g244130.m01	100	15352	154	4.70 (0.51)	3.15E-17	Protein TIFY 11A-Related
Bs.00g181270.m02[a]	74	6520	88	4.65 (0.49)	2.26E-16	Uncharacterized Protein
Bs.00g428250.m01	34	4864	142	4.64 (0.53)	5.42E-14	Extended Synaptotagmin-Related
Bs.00g512260.m01[i]	552	20157	37	4.63 (0.42)	9.41E-18	Glyoxalase/Fosfomycin Resistance/Dioxygenase Domain
Bs.00g228950.m01	2	333	207	4.56 (0.55)	1.44E-07	Dehydration-Responsive Element-Binding Protein 1a-Related
Bs.00g481180.m01	11	762	70	4.55 (0.46)	1.44E-15	Malectin-Like Carbohydrate-Binding Domain

	J01-S Untreated	J01-S 10 HAT				
Bs.00g122020.m01†	20	13981	683	6.76 (0.41)	3.41E-61	Uncharacterized Protein
Bs.00g016210.m01[j]	2	1874	811	6.29 (0.43)	2.46E-24	Precursor of CEP13/CEP14
Bs.00g176460.m01	7	1155	173	5.88 (0.39)	3.91E-32	At-Hook Motif Nuclear-Localized Protein 27
Bs.00g218880.m01	3	529	183	5.30 (0.43)	3.47E-17	D-Arabinono-1,4-Lactone Oxidase
Bs.00g168520.m01[k]	43	3475	80	5.23 (0.40)	6.91E-31	Cold Regulated Protein 27
Bs.00g168520.m02[k]	42	3334	78.7	5.08 (0.42)	1.54E-27	Cold Regulated Protein 27
Bs.00g176480.m01	1	295	511	5.07 (0.46)	6.62E-07	At-Hook Motif Nuclear-Localized Protein 27
Bs.00g239120.m01[k]	6	1088	176	4.96 (0.49)	3.49E-18	Aquaporin Tip3-1-Related
Bs.00g478760.m01[h]	2	793	457	4.70 (0.49)	3.96E-14	1-Aminocyclopropane-1-Carboxylate Synthase 4-Related
Bs.00g112620.m01	7	731	110	4.56 (0.47)	8.44E-17	Lipase/Lipooxygenase Domain
Bs.00g044610.m01[l]	263	9925	37.7	4.54 (0.35)	1.05E-29	Uncharacterized Protein
Bs.00g304090.m01[g]	154	4039	26.3	4.28 (0.31)	7.03E-32	AP2/ERF Domain
Bs.00g477580.m01[c]	279	45370	162	4.28 (0.50)	7.01E-23	Indole-3-Acetic Acid-Amido Synthetase GH3.2-Related
Bs.00g112710.m01	416	34778	83.5	4.24 (0.48)	7.24E-20	Lipoxygenase, C-Terminal
Bs.00g275080.m01	2	376	228	4.23 (0.48)	5.48E-11	Heme-Dependent Peroxidases
Bs.00g364070.m01	380	9639	25.4	4.22 (0.36)	2.28E-22	NAC Domain-Containing Protein 10-Related
Bs.00g422990.m01[d]	3600	120541	33.5	4.15 (0.40)	8.07E-20	4-Hydroxyphenylpyruvate Dioxygenase
Bs.00g359220.m02[n]	12	14262	1145	4.10 (0.58)	4.71E-22	Proteinase Inhibitor I13
Bs.00g520060.m01	448	8022	17.9	3.93 (0.24)	1.18E-46	B-Box Domain Protein 26-Related
Bs.00g058370.m01	1	152	131	3.92 (0.47)	3.23E-07	Metacaspase-4-Related

[a] Shared between J01-S 3 HAT and Flur-R 3 HAT top 20 upregulated genes
[c] Shared between 9425-S 10 HAT, J01-S 10 HAT and Flur-R 3/10 HAT top 20 upregulated genes
[d] Shared between J01-S 10 HAT and Flur-R 10 HAT top 20 upregulated genes
[g] Shared between 9425-S 3 HAT and J01-S 10 HAT top 20 upregulated genes
[h] Shared between 9425-S 3 HAT, Flur-R10 HAT and J01-S 10 HAT top 20 upregulated genes
[i] Shared between J01-S 3 HAT and 9425-S 3 HAT upregulated top 20
[j] Shared between 9425-S 10 HAT, Flur-R 3/10 HAT and J01-S 3 HAT/10 HAT top 20 upregulated genes

[k] Shared between 9425-S 10 HAT, Flur-R 10 HAT and J01-S 10 HAT top 20 upregulated genes
[l] Shared between 9245-S 3 HAT/10 HAT and J01-S 10 HAT top 20 upregulated genes
[n] Shared between 9425-S 10 HAT and J01-S 10 HAT top 20 upregulated genes
† Shared between J01-S 3 HAT /10 HAT top 20 upregulated genes

Table 5. Top 20 upregulated genes in fluroxypyr-susceptible kochia (*Bassia scoparia*) line 9425 at 3 h after treatment (HAT) and 10 HAT compared to the untreated timepoint. Fold change was calculated using the mean of normalized counts which was produced using the DESeq2 package in R. Log2 Fold Change was calculated in DESeq2, log2 fold change standard error and adjusted *p*-value were also calculated in DESeq2. The Wald-test obtained *p*-values were adjusted using the Benjamini-Hochberg method. The FDR was <0.05.

Gene ID	Mean of normalized counts		Fold Change	Log2 Fold Change (±SE)	P-value	Gene Description
	9425 Untreated	9425 3 HAT				
Bs.00g044610.m01[l]†	188	9324	50	4.69 (0.32)	3.31E-39	Uncharacterized Protein
Bs.00g301680.m01	973	17616	18	3.73 (0.27)	8.83E-32	Auxin-Responsive Protein IAA15
Bs.00g174320.m01†	39	664	17	3.36 (0.31)	6.95E-19	Histidine Kinase/HSP90-Like ATPase Superfamily
Bs.00g050510.m01	150	1971	13	3.36 (0.26)	1.40E-24	Cytochrome P450 734A1
Bs.00g229060.m01	84	2342	28	3.34 (0.41)	1.90E-11	Multi Antimicrobial Extrusion Protein/Protein Detoxification 50
Bs.00g107340.m01	474	5929	13	3.34 0.24)	5.55E-30	Auxin-Responsive Protein IAA1-Related
Bs.00g293750.m01	16	283	18	3.32 (0.34)	6.03E-14	Uncharacterized Protein
Bs.00g478760.m01[h]	7	583	83	3.31 (0.44)	3.80E-13	1-Aminocyclopropane-1-Carboxylate Synthase 4-Related
Bs.00g506330.m01	49	1128	23	3.27 (0.41)	4.61E-10	Chaperone J-Domain Superfamily
Bs.00g044350.m01	605	9804	16	3.14 (0.36)	7.06E-12	Uncharacterized Protein
Bs.00g512260.m01[i]	100	4635	46	3.13 (0.47)	1.83E-05	Lactoylglutathione Lyase Glyoxalase I
Bs.00g305330.m01	79	2260	29	3.06 (0.45)	5.39E-07	Cytochrome P450 76c1-Related
Bs.00g357520.m01	2	88	41	2.96 (0.42)	2.21E-07	Late Embryogenesis Abundant Protein
Bs.00g364640.m01	641	7072	11	2.94 (0.31)	4.70E-13	Signal Transduction Response Regulator, Receiver Domain
Bs.00g304090.m01[g]	196	2097	11	2.91 (0.30)	1.87E-14	AP2/ERF Transcription Factor ERF/PTI6
Bs.00g204690.m01	249	4008	16	2.90 (0.41)	1.21E-07	Zinc Finger, RING/FYVE/PHD-Type
Bs.00g048560.m01	768	8441	11	2.88 (0.31)	4.70E-13	Auxin-Responsive Protein IAA29
Bs.00g112660.m01	352	9548	27	2.87 (0.42)	7.59E-10	Linoleate 9S-Lipoxygenase 5, Chloroplastic
Bs.00g415260.m01	263	9451	36	2.86 (0.47)	3.22E-06	WRKY Transcription Factor 46-Related

Bs.00g290110.m01	336	3706	11	2.85 (0.35)	7.53E-10	Uncharacterized Protein
	9425 Untreated	9425 10 HAT				
Bs.00g427230.m01	28	5143	183	6.20	1.09E-37	Member of 'GDXG' Family of Lipolytic Enzymes
Bs.00g168520.m01[k]	46	4282	94	5.64	6.80E-40	Cold Regulated Protein 27
Bs.00g168520.m02[k]	53	4276	81	5.44	1.36E-35	Cold Regulated Protein 27
Bs.00g174320.m01†	39	2571	66	5.40	1.17E-53	Histidine Kinase/HSP90-Like ATPase Superfamily
Bs.00g044610.m01[l] †	188	10766	57	5.07	3.35E-49	Uncharacterized Protein
Bs.00g261820.m01	0	77	77	4.93	4.95E-07	Pectin Lyase Fold/Virulence Factor
Bs.00g016210.m01[j]	2	1675	988	4.87	9.19E-22	Precursor of CEP13/CEP14
Bs.00g413330.m01	620	71783	116	4.85	4.01E-22	Cystathionine Gamma-Lyase
Bs.00g148640.m01[m]	660	27633	42	4.71	1.26E-34	2-Oxoisovalerate Dehydrogenase Subunit Alpha 2, Mitochondrial
Bs.00g305280.m01	0	52	52	4.65	1.41E-05	Allergen V5/TPX-1-Related, Conserved Site
Bs.00g142300.m01	0	48	48	4.58	2.08E-05	Pectin Lyase Fold/Virulence Factor
Bs.00g477660.m01	9	4426	510	4.56	1.47E-25	Gibberellin-Regulated GASA/GAST/SNAKIN Family Protein-Related
Bs.00g359220.m02[n]	41	15538	383	4.56	1.16E-25	Proteinase Inhibitor I13, Potato Inhibitor I Superfamily
Bs.00g239120.m01[k]	2	1207	619	4.54	5.71E-14	Aquaporin TIP3-1-Related
Bs.00g208750.m01	287	11553	40	4.52	1.72E-25	CASP-Like Protein 1E1-Related
Bs.00g430360.m01	60	2663	44	4.44	7.76E-24	Protein Early Flowering 4
Bs.00g100040.m01	3	789	228	4.43	5.81E-09	Bet V I/Major Latex Protein
Bs.00g477580.m01[c]	92	39708	431	4.41	8.98E-30	Indole-3-Acetic Acid-Amido Synthetase GH3.2-Related
Bs.00g526000.m01	228	9711	43	4.40	4.47E-21	NAC Domain
Bs.00g447890.m01	0	73	73	4.36	6.43E-07	Pectinesterase

[c] Shared between 9425-S 10 HAT, J01-S 10 HAT and Flur-R 3 HAT/10 HAT top 20 upregulated genes
[g] Shared between 9425-S 3 HAT and J01-S 10 HAT top 20 upregulated genes

[h] Shared between 9425-S 3 HAT, Flur-R 10 HAT and J01-S 10 HAT top 20 upregulated genes
[I] Shared between 9425-S 3 HAT and J01-S 3 HAT top 20 upregulated genes
[j] Shared between 9425-S 10 HAT, Flur-R 3 HAT /10 HAT and J01-S 3 HAT/10 HAT top 20 upregulated genes
[k] Shared between 9425-S 10 HAT, Flur-R 10 HAT and J01-S 10 HAT top 20 upregulated genes
[l] Shared between 9245-S 3 HAT/10 HAT and J01-S 10 HAT top 20 upregulated genes
[m] Shared between 9425-S 10 HAT and Flur-R 10 HAT top 20 upregulated genes
[n] Shared between 9425-S 10 HAT and J01-S 10 HAT top 20 upregulated genes
† Shared between 9425-S 3 HAT/10 HAT top 20 upregulated genes

Table 6. Top 20 downregulated genes in fluroxypyr resistant kochia (*Bassia scoparia*) line Flur-R at 3 h after treatment (HAT) and 10 HAT compared to the untreated timepoint. Fold change was calculated using the mean of normalized counts which was produced using the DESeq2 package in R. Log2 Fold Change was calculated in DESeq2, log2 fold change standard error and adjusted *p*-value were also calculated in DESeq2. The Wald-test obtained *p* values were adjusted using the Benjamini-Hochberg method. The FDR was <0.05.

Gene ID	Mean of normalized counts		Fold Change	Log2 Fold Change (±SE)	Pvalue	Gene Description
	Flur-R Untreated	Flur-R 3 HAT				
Bs.00g258890.m01†	136	2	-66	-3.96 (0.44)	5.28E-11	LRR
Bs.00g104620.m01[e] †	7356	172	-43	-3.64 (0.43)	4.34E-13	Protein Kinase
Bs.00g354480.m01[r]	4017	217	-19	-3.35 (0.37)	4.39E-13	SAM Dependent Carboxyl Methyltransferase
Bs.00g370120.m01[r]	197	7	-29	-3.19 (0.45)	2.63E-08	Lipid Binding Domain
Bs.00g362240.m01	574	29	-20	-3.16 (0.42)	7.22E-09	Bicarbonate Transporter
Bs.00g195790.m01[b]	234	10	-24	-3.10 (0.44)	2.63E-08	Proton Dependent Oligopeptide Transporter
Bs.00g056860.m01	127	1	-95	-3.01 (0.48)	1.48E-06	Peptidase/Proteinase Inhibitor I9
Bs.00g119650.m01	1565	66	-24	-2.97 (0.44)	4.39E-08	Nicotianamine Synthase
Bs.00g251440.m01[r]	687	51	-13	-2.97 (0.37)	3.33E-10	Multicopper Oxidase
Bs.00g126000.m01 †	66186	1694	-39	-2.94 (0.47)	3.76E-08	NADH Cytochrome B5 Reductase
Bs.00g123470.m01	475	38	-13	-2.92 (0.37)	3.95E-10	Glycoside Hydrolase
Bs.00g264170.m01[r]	5895	687	-9	-2.87 (0.23)	6.32E-23	Glycoside Hydrolase
Bs.00g195800.m01	205	14	-15	-2.82 (0.42)	3.44E-07	Proton Dependent Oligopeptide Transporter
Bs.00g403960.m01 †	36087	2902	-12	-2.75 (0.39)	1.81E-08	Carotenoid Oxygenase
Bs.00g528960.m01[r]	1273	96	-13	-2.73 (0.40)	1.24E-07	Auxin-Inducible
Bs.00g348080.m01	965	77	-13	-2.73 (0.40)	9.58E-08	Uncharacterized Protein
Bs.00g420960.m01[p]	1713	12	-148	-2.65 (049)	1.28E-08	Chlorophyll A-B Binding Protein
Bs.00g421070.m01[p]	2101	12	-177	-2.63 (0.49)	4.44E-09	Chlorophyll A-B Binding Protein
Bs.00g429620.m01	67	4	-16	-2.63 (0.44)	2.53E-05	Multicopper Oxidase
Bs.00g372170.m02	220	11	-20	-2.62 (0.46)	6.13E-06	Uncharacterized Protein
	Flur-R Untreated	Flur-R 10 HAT				

Bs.00g253530.m01[u]	3988	31	-131	-6.56 (0.29)	2.06E-91	Tetratricopeptide-Like Helical Domain Superfamily
Bs.00g240870.m01[u]	389614	3606	-108	-6.40 (0.26)	1.25E-104	Chlorophyll A-B Binding Protein
Bs.00g240870.m02[u]	246956	2360	-105	-6.35 (0.27)	5.04E-101	Chlorophyll A-B Binding Protein
Bs.00g060850.m01[u]	59810	959	-62	-5.34 (0.36)	1.12E-37	Thiamine Thiazole Synthase
Bs.00g126000.m01†	66186	447	-148	-5.12 (0.50)	4.64E-19	NADH-Cytochrome B5 Reductase
Bs.00g258890.m01†	136	1	-126	-5.10 (0.48)	1.28E-14	Tyrosine-Protein Kinase, Active Site
Bs.00g205780.m01	1166	26	-44	-4.99 (0.32)	8.66E-41	Cytochrome P450 90A1
Bs.00g133350.m02	459	11	-44	-4.88 (0.34)	8.43E-35	Serine Protease Family S10 Serine Carboxypeptidase
Bs.00g104620.m01[e]†	7356	100	-73	-4.81 (0.45)	7.39E-21	Phosphoenolpyruvate Carboxylase Kinase 1-Related
Bs.00g133350.m01	507	12	-41	-4.69 (0.36)	3.06E-28	Peptidase S10, Serine Carboxypeptidase
Bs.00g192330.m01	293420	9287	-32	-4.60 (0.31)	1.24E-37	Magnesium-Chelatase, Subunit H
Bs.00g279710.m01[f]	7847	165	-48	-4.59 (0.42)	6.82E-20	Aerolysin-Like Toxin
Bs.00g299020.m01	794	16	-50	-4.58 (0.44)	9.29E-19	O-Acyltransferase WSD1
Bs.00g116620.m01	2862	91	-31	-4.54 (0.31)	2.96E-37	Coenzyme Q-Binding Protein Coq10
Bs.00g480400.m01[v]	498	8	-62	-4.52 (0.49)	4.12E-14	Plc-Like Phosphodiesterase
Bs.00g206320.m01	10980	18	-609	-4.48 (0.58)	5.73E-15	Cytochrome P450 Superfamily
Bs.00g058520.m01[u]	1710	65	-26	-4.47 (0.26)	1.29E-47	Acyl-CoA N-Acyltransferases
Bs.00g205800.m01	868	23	-38	-4.45 (0.41)	1.42E-19	Cytochrome P450 90A1
Bs.00g403960.m01†	36087	952	-38	-4.45 (0.38)	4.49E-23	Carotenoid Cleavage Dioxygenase 4, Chloroplastic-Related
Bs.00g471400.m01	279	6	-43	-4.44 (0.43)	3.69E-17	Voltage-gated potassium channels

[b] Shared between J01-S 3 HAT and Flur-R 3 HAT top 20 downregulated genes
[e] Shared between J01-S 3 HAT and Flur-R 3 HAT/10 HAT top 20 downregulated genes
[f] Shared between J01-S 10 HAT and Flur-R 10 HAT top 20 downregulated genes
[p] Shared between 9425-S 3 HAT, J01-S 3 HAT and Flur-R 3 HAT top 20 downregulated genes
[r] Shared between 9425-S 3 HAT and Flur-R 3 HAT top 20 downregulated genes
[v] Shared between 9425-S 10 HAT and Flur-R 10 HAT top 20 downregulated genes

† Shared between Flur-R 3 HAT/10 HAT top 20 downregulated genes

Table 7. Top 20 downregulated genes in fluroxypyr susceptible kochia (*Bassia scoparia*) line J01-S at 3 h after treatment (HAT) and 10 HAT compared to the untreated timepoint. Fold change was calculated using the mean of normalized counts which was produced using the DESeq2 package in R. Log2 Fold Change was calculated in DESeq2, log2 fold change standard error and adjusted *p*-value were also calculated in DESeq2. The Wald-test obtained *p*-values were adjusted using the Benjamini-Hochberg method. The FDR was <0.05.

Gene ID	Mean of normalized counts		Fold Change	Log2 Fold Change (±SE)	P-value	Gene Description
	J01-S Untreated	J01-S 3 HAT				
Bs.00g420960.m01[p]	2805	114	-25	-7.08 (0.43)	3.21E-37	Early Light-Induced Protein 1, Chloroplastic-Related
Bs.00g421070.m01[p]	3659	129	-28	-6.40 (0.46)	1.24E-31	Early Light-Induced Protein 1, Chloroplastic-Related
Bs.00g104620.m01[e]†	6485	87	-74	-5.07 (0.37)	1.81E-33	Phosphoenolpyruvate Carboxylase Kinase 1-Related
Bs.00g518390.m01[o]	1330	91	-15	-4.38 (0.45)	8.59E-17	Chalcone/Stilbene Synthase
Bs.00g383340.m01[q]†	62541	614	-102	-4.23 (0.38)	5.29E-22	S-Adenosyl-L-Methionine-Dependent Methyltransferase
Bs.00g383340.m02[q]†	63412	627	-101	-4.22 (0.38)	6.99E-22	S-Adenosyl-L-Methionine-Dependent Methyltransferase
Bs.00g479050.m01	1337	71	-19	-4.00 (0.37)	2.08E-19	Multicopper Oxidase, Type 1, 2, 3
Bs.00g150590.m01	19150	874	-22	-3.52 (0.23)	6.20E-37	Carboxyvinyl-Carboxyphosphonate Phosphorylmutase, Chloroplastic
Bs.00g417520.m01	3342	727	-5	-3.51 (0.46)	1.48E-09	Cytochrome P450 86a7
Bs.00g196880.m01	12374	621	-20	-3.40 (0.29)	7.21E-22	Haloacid Dehalogenase-Like Hydrolase Domain-Containing Protein
Bs.00g228740.m01	3131	464	-7	-3.36 (0.43)	4.71E-10	Glucose-Methanol-Choline Oxidoreductase
Bs.00g488230.m02[s]	493	30	-16	-3.27 (0.39)	4.26E-11	BTB/POZ Domain-Containing Protein Dot3
Bs.00g091650.m01	5414	1641	-3	-3.24 (0.40)	1.94E-10	Cytochrome P450 77A4-Related
Bs.00g179870.m01	560	21	-27	-3.20 (0.48)	1.00E-07	Thioredoxin-LIK
Bs.00g488230.m01[s]	589	39	-15	-3.15 (0.38)	3.15E-11	BTB/POZ Domain-Containing Protein DOT3
Bs.00g124100.m01	25716	1786	-14	-3.14 (0.37)	1.34E-11	Multi Antimicrobial Extrusion Protein
Bs.00g195790.m01[b]	661	34	-20	-3.11 (0.53)	1.62E-06	Proton-Dependent Oligopeptide Transporter Family

Bs.00g247060.m01	1115	125	-9	-3.08 (0.36)	3.19E-11	Major Facilitator Protein
Bs.00g418430.m01	2076	95	-22	-3.05 (0.24)	3.85E-24	Peptidase S10, Serine Carboxypeptidase
Bs.00g310680.m01	4294	815	-5	3.02 (0.39)	3.14E-09	Aquaporin transporter
	J01-S Untreated	J01-S 10 HAT				
Bs.00g237950.m01	31050	185	-168	-6.11 (0.47)	2.24E-29	Purine and Uridine Phosphorylases
Bs.00g383340.m01[q]†	62541	614	-102	-5.98 (0.34)	5.59E-55	S-Adenosyl-L-Methionine-Dependent Methyltransferase
Bs.00g383340.m02[q]†	63412	627	-101	-5.97 (0.34)	7.93E-55	S-Adenosyl-L-Methionine-Dependent Methyltransferase
Bs.00g060850.m01[u]	61097	963	-63	-5.71 (0.25)	7.00E-96	Thiamine Thiazole Synthase
Bs.00g253530.m01[u]	3380	51	-66	-5.61 (0.30)	2.91E-59	Tetratricopeptide-Like Helical Domain Superfamily
Bs.00g104620.m01[e]†	6485	87	-74	-5.57 (0.33)	7.03E-51	Phosphoenolpyruvate Carboxylase Kinase 1-Related
Bs.00g002550.m01[t]	6898	56	-123	-5.53 (0.50)	1.28E-19	Glucose-6-Phosphate/Phosphate Translocator 2, Chloroplastic
Bs.00g058520.m01[u]	2423	35	-69	-5.51 (0.36)	1.50E-39	Acyl-CoA N-Acyltransferase
Bs.00g279710.m01[f]	25350	388	-65	-5.38 (0.41)	1.01E-26	Aerolysin-Like Toxin
Bs.00g240870.m01[u]	407872	5349	-76	-5.26 (0.45)	3.48E-22	Chlorophyll A-B Binding Protein
Bs.00g240870.m02[u]	265402	3480	-76	-5.24 (0.46)	1.70E-21	Chlorophyll A-B Binding Protein
Bs.00g236450.m01	13388	387	-35	-4.88 (0.24)	4.84E-72	Protein Proton Gradient Regulation 5
Bs.00g115330.m01	71272	1829	-39	-4.85 (0.34)	7.75E-34	Photosystem I Reaction Center Subunit Iv A, Chloroplastic-Related
Bs.00g020870.m01	209812	6578	-32	-4.69 (0.28)	3.26E-46	Chlorophyll A/B Binding Protein
Bs.00g412900.m01	18823	572	-33	-4.65 (0.31)	1.54E-39	Granule-Bound Starch Synthase 1, Chloroplastic/Amyloplastic
Bs.00g476760.m01	699	11	-62	-4.63 (0.50)	4.10E-14	Z -3-Hexen-1-Ol Acetyltransferase
Bs.00g527540.m01	7607	68	-112	-4.47 (0.58)	7.97E-10	Proteinase Inhibitor I3, Kunitz Legume
Bs.00g472680.m01	1623	58	-28	-4.35 (0.36)	3.49E-23	Uncharacterized Protein
Bs.00g383860.m01	33142	1574	-21	-4.31 (0.15)	7.02E-130	Fructose-1,6-Bisphosphatase-Related
Bs.00g055990.m01	635	21	-30	-4.28 (0.40)	3.67E-19	Uncharacterized Protein

[b] Shared between J01-S 3 HAT and Flur-R 3 HAT top 20 downregulated genes

[e] Shared between 9425-S 3 HAT, J01-S 3 HAT/10 HAT and Flur-R 3 HAT/10 HAT top 20 downregulated genes
[f] Shared between J01-S 10 HAT and Flur-R 10 HAT top 20 downregulated genes
[o] Shared between 9425-S 3 HAT/10 HAT and J01-S 3 HAT top 20 downregulated genes
[p] Shared between 9425-S 3 HAT, J01-S 3 HAT and Flur-R 3 HAT top 20 downregulated genes
[q] Shared between 9425-S 3 HAT and J01-S 3 HAT/10 HAT top 20 downregulated genes
[s] Shared between 9425-S 3 HAT and J01-S 3 HAT top 20 downregulated genes
[t] Shared between 9425-S 10 HAT and J01-S 10 HAT top 20 downregulated genes
[u] Shared between 9425-S 10 HAT, J01-10 HAT, Flur-R 10 HAT top 20 downregulated genes
[w] Shared between 9425-S 10 HAT and J01-S 3 HAT top 20 downregulated genes

Table 8. Top 20 downregulated genes in fluroxypyr susceptible kochia (*Bassia scoparia*) line 9425 at 3 hours after treatment (HAT) and 10HAT compared to the untreated timepoint. Fold change was calculated using the mean of normalized counts which was produced using the DESeq2 package in R. Log2 Fold Change was calculated in DESeq2, log2 fold change standard error and adjusted *p*-value were also calculated in DESeq2. The Wald-test obtained *p*-values were adjusted using the Benjamini-Hochberg method. The FDR was <0.05.

Gene ID	Mean of normalized counts		Fold Change	Log2 Fold Change (±SE)	Pvalue	Gene Description
	9425 Untreated	9425 3 HAT				
Bs.00g518390.m01[o]†	4504	68	67	-5.06	1.80E-41	Chalcone/Stilbene Synthase
Bs.00g421070.m01[p]	1918	8	238	-3.69	1.06E-14	Early Light-Induced Protein 1, Chloroplastic-Related
Bs.00g420960.m01[p]	1557	7	210	-3.61	9.55E-14	Early Light-Induced Protein 1, Chloroplastic-Related
Bs.00g543360.m01	2375	98	24	-3.38	1.15E-11	Oxoglutarate/Iron-Dependent Dioxygenase
Bs.00g383340.m01[q]	13230	691	19	-3.31	1.70E-12	S-Adenosyl-L-Methionine-Dependent Methyltransferase
Bs.00g383340.m02[q]	13404	701	19	-3.31	1.82E-12	S-Adenosyl-L-Methionine-Dependent Methyltransferase
Bs.00g354480.m01[r]	1542	87	18	-3.25	1.69E-11	S-Adenosyl-L-Methionine-Dependent Methyltransferase
Bs.00g370120.m01[r]	364	8	45	-3.20	6.65E-09	CRAL-TRIO Lipid Binding Domain
Bs.00g268300.m01†	724	5	140	-3.16	2.50E-10	Early Light-Induced Protein 1, Chloroplastic-Related
Bs.00g364920.m01	453	37	12	-3.13	1.87E-15	Serine-Threonine/Tyrosine-Protein Kinase, Catalytic Domain
Bs.00g488230.m01[s]	532	38	14	-3.11	2.63E-12	BTB/POZ Domain-Containing Protein DOT3
Bs.00g488230.m02[s]	447	37	12	-3.02	1.55E-12	BTB/POZ Domain-Containing Protein DOT3
Bs.00g475340.m01	478	38	13	-2.95	1.42E-09	Camp-Response Element Binding Protein-Related
Bs.00g528960.m01[r]	880	51	17	-2.89	1.17E-07	Auxin_Inducible
Bs.00g180610.m01	1127	60	19	-2.86	1.87E-07	Glycoside Hydrolase Family 1
Bs.00g251440.m01[r]	1535	140	11	-2.81	4.78E-10	Multicopper Oxidase, Type 2
Bs.00g396960.m01	646	57	11	-2.70	3.62E-08	UDP-Glycosyltransferase/Glycogen

						Phosphorylase
Bs.00g420270.m01	1575	133	12	-2.67	2.39E-06	Glucose-Methanol-Choline Oxidoreductase
Bs.00g104620.m01[e]	1497	106	14	-2.67	9.72E-07	Serine/Threonine-Protein Kinase
Bs.00g264170.m01[r]	11365	1301	9	-2.66	1.13E-10	Beta-Glucosidase 1-Related
	9425-S Untreated	9425 10 HAT				
Bs.00g002550.m01[t]	10014	41	242	-6.95	3.36E-47	Glucose-6-Phosphate/Phosphate Translocator 2, Chloroplastic
Bs.00g518390.m01[o]†	4504	21	213	-6.94	7.61E-75	Chalcone/Stilbene Synthase, C-Terminal
Bs.00g240870.m01[u]	419016	3501	120	-6.09	2.32E-35	Chlorophyll A-B Binding Protein
Bs.00g240870.m02[u]	274431	2301	119	-6.09	4.32E-35	Chlorophyll A-B Binding Protein
Bs.00g058520.m01[u]	3828	37	103	-6.08	4.85E-49	Acyl-CoA N-Acyltransferase
Bs.00g060850.m01[u]	105278	1179	89	-5.75	2.70E-36	Thiamine Thiazole Synthase
Bs.00g253530.m01[u]	3725	49	76	-5.63	1.99E-37	Tetratricopeptide-Like Helical Domain Superfamily
Bs.00g535160.m01	480	4	110	-5.57	2.65E-21	WAT1-Related Protein
Bs.00g124870.m01	18471	116	160	-5.33	8.61E-16	Lipoxygenase
Bs.00g480400.m01[v]	684	8	85	-5.33	1.31E-20	PLC-Like Phosphodiesterase
Bs.00g418430.m01	3350	46	73	-5.33	6.52E-27	Peptidase S10, Serine Carboxypeptidase
Bs.00g535430.m01	143	1	108	-5.30	7.70E-15	Cyclin_A_B_D_E
Bs.00g518030.m01	721	2	412	-5.13	1.43E-12	Chalcone/Stilbene Synthase, Polyketide Synthase, Type III, Hydroxymethylglutaryl-CoA Synthase
Bs.00g055200.m01	754	15	51	-5.06	7.48E-28	Glyceraldehyde-3-Phosphate Dehydrogenase-Like
Bs.00g535430.m02	121	1	92	-5.05	2.97E-13	Cyclin_A_B_D_E
Bs.00g249240.m01	212	2	117	-5.02	5.87E-13	Uncharacterized Protein
Bs.00g268300.m01†	724	4	171	-5.01	6.54E-14	Early Light-Induced Protein 1
Bs.00g435140.m01	1573	29	55	-4.95	4.56E-22	Proton-Dependent Oligopeptide Transporter Family
Bs.00g136920.m01	1931	16	123	-4.92	1.48E-13	Cupin_1
Bs.00g478150.m01	781	6	138	-4.90	1.45E-11	Glycoside Hydrolase Family 17

[e] Shared between 9425 3 HAT, J01-3 HAT/10 HAT and Flur-R 3 HAT/10 HAT top 20 downregulated genes
[o] Shared between 9425-S 3 HAT/10 HAT and J01-S 3 HAT top 20 downregulated genes
[p] Shared between 9425-S 3 HAT, J01-S 3 HAT and Flur-R 3 HAT top 20 downregulated genes
[q] Shared between 9425-S 3 HAT and J01-S 3 HAT/10 HAT top 20 downregulated genes
[r] Shared between 9425-S 3 HAT and Flur-R 3 HAT top 20 downregulated genes
[s] Shared between 9425-S 3 HAT and J01-S 3 HAT top 20 downregulated genes
[t] Shared between 9425-S 10 HAT and J01-S 10 HAT top 20 downregulated genes
[v] Shared between 9425-S 10 HAT and Flur-R 10 HAT top 20 downregulated genes
[w] Shared between 9425-S 10 HAT and J01-S 3 HAT top 20 downregulated genes
†Shared between 9425-S 3 HAT and 10 HAT top 20 downregulated genes